Technical Document 1600
August 1989

Atmospheric Horizontal-Inhomogeneity Effects on the Optical Depths Determined by the Double-Elevation-Angle Lidar Technique

Merle R. Paulson

NAVAL OCEAN SYSTEMS CENTER

San Diego, California 92152-5000

E. G. SCHWEIZER, CAPT, USN
Commander

R. M. HILLYER
Technical Director

ADMINISTRATIVE INFORMATION

The work described in this document was performed from April 1989 to July 1989 by the Tropospheric Branch, Code 543, Naval Ocean Systems Center (NOSC), for NOSC Code 402, Command and Control Department.

Released by
H. V. Hitney, Head
Tropospheric Branch

Under authority of
J. H. Richter, Head
Ocean and Atmospheric
Sciences Division

REPORT DOCUMENTATION PAGE

1a. REPORT SECURITY CLASSIFICATION UNCLASSIFIED	1b. RESTRICTIVE MARKINGS
2a. SECURITY CLASSIFICATION AUTHORITY	3. DISTRIBUTION/AVAILABILITY OF REPORT
2b. DECLASSIFICATION/DOWNGRADING SCHEDULE	Approved for public release; distribution is unlimited.
4. PERFORMING ORGANIZATION REPORT NUMBER(S) NOSC TD 1600	5. MONITORING ORGANIZATION REPORT NUMBER(S)
6a. NAME OF PERFORMING ORGANIZATION Naval Ocean Systems Center 6b. OFFICE SYMBOL (if applicable) Code 543	7a. NAME OF MONITORING ORGANIZATION
6c. ADDRESS (City, State and ZIP Code) San Diego, CA 92152-5000	7b. ADDRESS (City, State and ZIP Code)
8a. NAME OF FUNDING/SPONSORING ORGANIZATION Naval Ocean Systems Center 8b. OFFICE SYMBOL (if applicable) Code 402	9. PROCUREMENT INSTRUMENT IDENTIFICATION NUMBER
8c. ADDRESS (City, State and ZIP Code) San Diego, CA 92152-5000	10. SOURCE OF FUNDING NUMBERS PROGRAM ELEMENT NO. 62435N PROJECT NO. RM35G80 TASK NO. N02C AGENCY ACCESSION NO. 540-CDB6

11. TITLE (Include Security Classification)

ATMOSPHERIC HORIZONTAL-INHOMOGENEITY EFFECTS ON THE OPTICAL DEPTHS DETERMINED BY THE DOUBLE-EVALUATION-ANGLE LIDAR TECHNIQUE

12. PERSONAL AUTHOR(S)

Merle R. Paulson

13a. TYPE OF REPORT	13b. TIME COVERED	14. DATE OF REPORT (Year, Month, Day)	15. PAGE COUNT
Final	FROM Apr 1989 TO Jul 1989	August 1989	35

16. SUPPLEMENTARY NOTATION

17. COSATI CODES			18. SUBJECT TERMS (Continue on reverse if necessary and identify by block number)
FIELD	GROUP	SUB-GROUP	lidar extinction coefficients integrated extinction and visibility

19. ABSTRACT (Continue on reverse if necessary and identify by block number)

This report considers the proposals of dual, or multiple, elevation-angle lidar measurements to determine integrated extinction, or optical depth, in the vertical. Atmospheric conditions have to be horizontally homogeneous for this to be a usable technique. Additionally, the ratio of backscatter coefficient to extinction coefficient must be constant over the height range of interest. The results indicate that this is not a usable technique, since the atmosphere is not sufficiently horizontally homogeneous.

20. DISTRIBUTION/AVAILABILITY OF ABSTRACT	21. ABSTRACT SECURITY CLASSIFICATION
☐ UNCLASSIFIED/UNLIMITED ☒ SAME AS RPT ☐ DTIC USERS	UNCLASSIFIED

22a. NAME OF RESPONSIBLE PERSON	22b. TELEPHONE (Include Area Code)	22c. OFFICE SYMBOL
Merle R. Paulson	(619) 553-1413	Code 543

CONTENTS

INTRODUCTION

The Navy has been looking for a reliable and accurate method for measuring optical depth, or visibility, for quite a few years. The lidar has been suggested as a possible tool to do this (Lentz, 1982). Single-lidar techniques, however, suffer from the difficulty of having two unknowns, but only one equation. Inversion techniques have been proposed to try to avoid this limitation (Klett, 1981,1985). These techniques require that some assumptions be made about atmospheric conditions. Among the most common of these assumptions are that the atmospheric conditions are horizontally homogeneous and that the backscatter-to-extinction ratio is a constant.

Some scientists have used multiple-elevation-angle range-corrected lidar returns, $S(R)$, to determine the integrated optical extinction in the vertical direction (Spinhirne et al., 1980; Russell and Livingston, 1984). In order for this to be a useful method, the atmosphere must be horizontally homogeneous, a condition that frequently does not exist. Russell and Livingston say that both they and Spinhirne et al. have found that, within the convective layer, the atmospheric backscattering coefficient rarely if ever has the degree of horizontal homogeneity required. Additionally, both the transmitted power and the backscattered lidar signal must be accurately measured.

The use of this method to get optical depth in the vertical has recently been suggested by Kunz (1988), so it was thought worthwhile to take another look at it.

Rarely, if ever, is horizontal homogeneity found in the San Diego area. In fact, in some cases the degree of inhomogeneity is very pronounced (Paulson, 1986). Even though this is true, some measurements will be made using this technique to see what the results might look like.

MATHEMATICAL DERIVATION

For purposes of this study, assume the atmosphere to be horizontally homogeneous with an extinction coefficient, $\sigma(h)$, that varies only in the vertical direction. In Fig. 1 ϕ_1 and ϕ_2 are the elevation angles for lidars 1 and 2, respectively.

For a vertical lidar shot ($\phi_1 = \phi_2 = 90$ degrees) the power received from a scattering element at height h is determined from the single-scatter lidar equation to be

$$P(h) = \frac{C\beta(h)}{h^2} \exp\left[-2\int_0^h \sigma(h')dh'\right] \tag{1}$$

where $\beta(h)$ is the backscatter coefficient and C is the instrumentation constant. Then the power received from an altitude h_1 along a slant path R_1 elevated ϕ_1 degrees is $P(R_1)$ and along a slant path R_2 elevated ϕ_2 degrees is $P(R_2)$ where

$$P(R_1) = \frac{C\beta(h_1)}{(h_1 \sin\phi_1)^2} \exp\left[-2\int_0^{h_1} \sigma(h')dh' \sin\phi_1\right] \tag{2}$$

and

$$P(R_2) = \frac{C\beta(h_1)}{(h_1 \sin\phi_2)^2} \exp\left[-2\int_0^{h_1} \sigma(h')dh' \sin\phi_2\right] \tag{3}$$

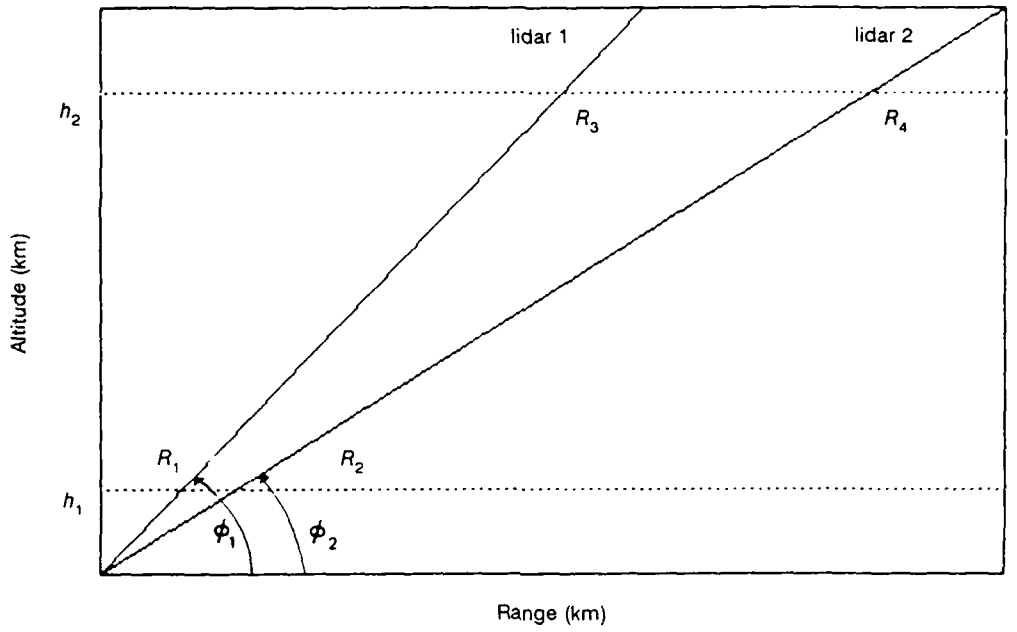

Figure 1. Geometry for two-elevation-angle lidar measurements.

Dividing Eq. 2 by Eq. 3 we get

$$\frac{P(R_1)(h_1 \sin\phi_1)^2}{P(R_2)(h_1 \sin\phi_2)^2} = \exp\left\{-2\left[\frac{1}{\sin\phi_1} - \frac{1}{\sin\phi_2}\right]\int_0^{h_1}\sigma(h')dh'\right\} \tag{4}$$

or, taking the logarithm of both sides

$$\ln\left[\frac{P(R_1)(h_1 \sin\phi_1)^2}{P(R_2)(h_1 \sin\phi_2)^2}\right] = 2\left[\frac{1}{\sin\phi_1} - \frac{1}{\sin\phi_2}\right]\int_0^{h_1}\sigma(h')dh' \tag{5}$$

and

$$\int_0^{h_1}\sigma(h')dh' = \frac{S(R_1) - S(R_2)}{2(1 \sin\phi_2 - 1 \sin\phi_1)} \tag{6}$$

where

$$S(R) = \ln[P(R)(h \sin\phi)^2] \tag{7}$$

Similarly

$$\int_0^{h_2}\sigma(h')dh' = \frac{S(R_3) \quad S(R_4)}{2(1 \sin\phi_2 \quad 1 \sin\phi_1)} \tag{8}$$

Then

$$\int_{h_1}^{h_2} \sigma(h')dh' = \int_0^{h_2} \sigma(h')dh' - \int_0^{h_1} \sigma(h')dh'$$

$$= \frac{[S(R_3) - S(R_4)] - [S(R_1) - S(R_2)]}{2(1 \sin\phi_2 - 1 \sin\phi_1)} \tag{9}$$

MEASUREMENT PROCEDURE

Data were taken on May 17, 1989, while there was a thin overcast layer at about 500 meters. A second set of data was taken on May 24, 1989. At this time there was a moderate inversion at about 300 meters.

Two visioceilometer lidars were used (Lentz, 1982). A 24-volt dc power supply had been added to each lidar to improve stability. The lidars were set up at building 323 on the west side of Point Loma and pointed west overlooking the Pacific Ocean. They were aligned so that the horizontal cross hair of each lidar was on the horizon. The vertical cross hairs were aligned on the mast of a sailboat 3 or 4 km away. This assured that the two lidars were looking at very nearly the same horizontal path. A series of nearly simultaneous shots were made with this arrangement. Next, without changing the orientation, the elevation angle of lidar 1 was increased to 25 degrees and that of lidar 2 was increased to 50 degrees. A series of nearly simultaneous shots were made with this configuration.

An example of the horizontal shots taken on May 24 is shown in Fig. 2. The two lidars show quite good agreement. The irregularities observed at close range are probably a result of on-shore winds striking the bluff and rising.

The $S(R)$ data were plotted as a function of altitude for the two-angle measurements. Figure 3 is an example of these, showing data set 9 for May 17. Figure 4 is the same thing for data set 8 on May 24. $S(R)$ versus altitude plots for other data sets are shown in the Appendix.

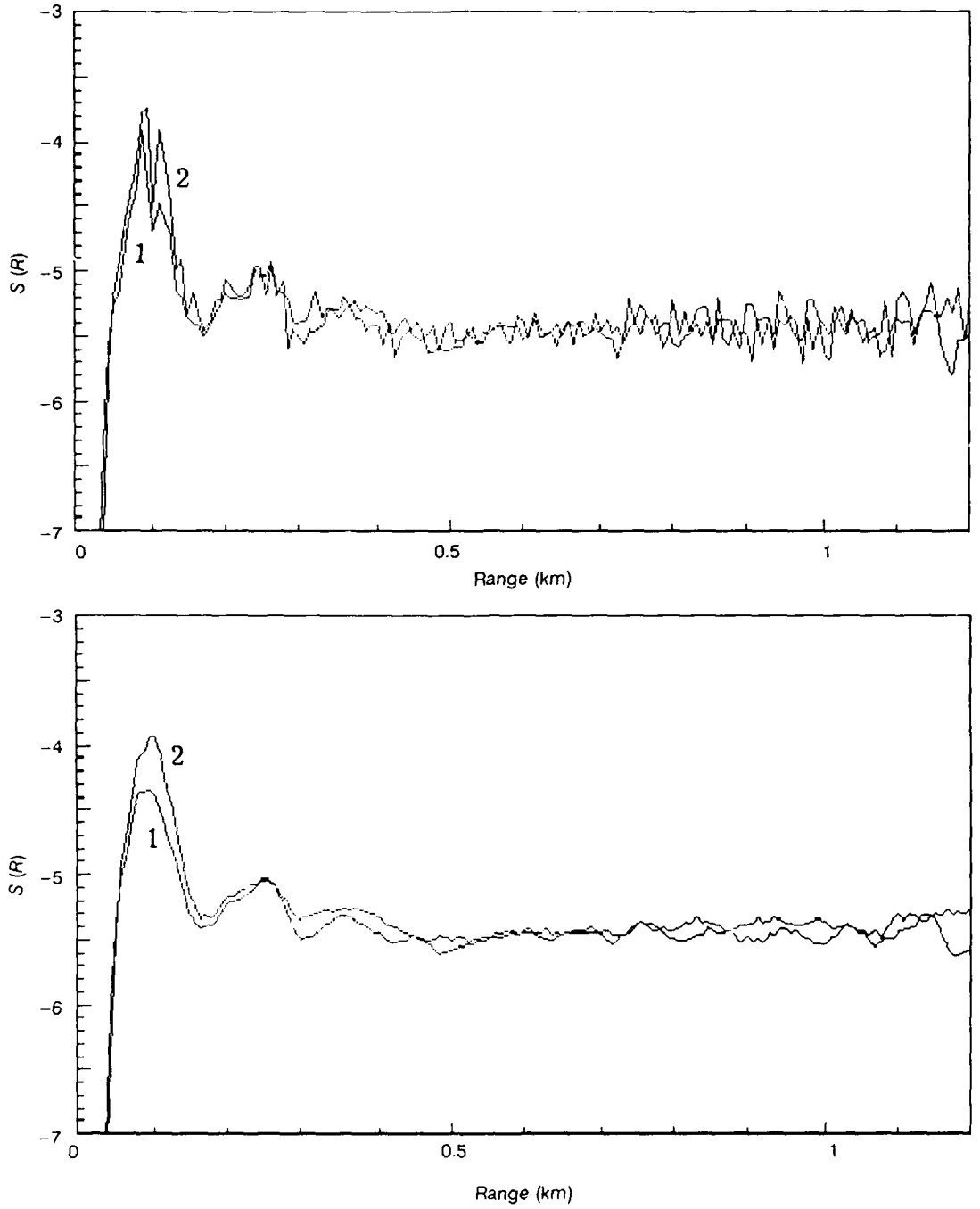

Figure 2. An example of parallel horizontal lidar shots. Upper graph is for no averaging and lower graph is for a 5-point running average.

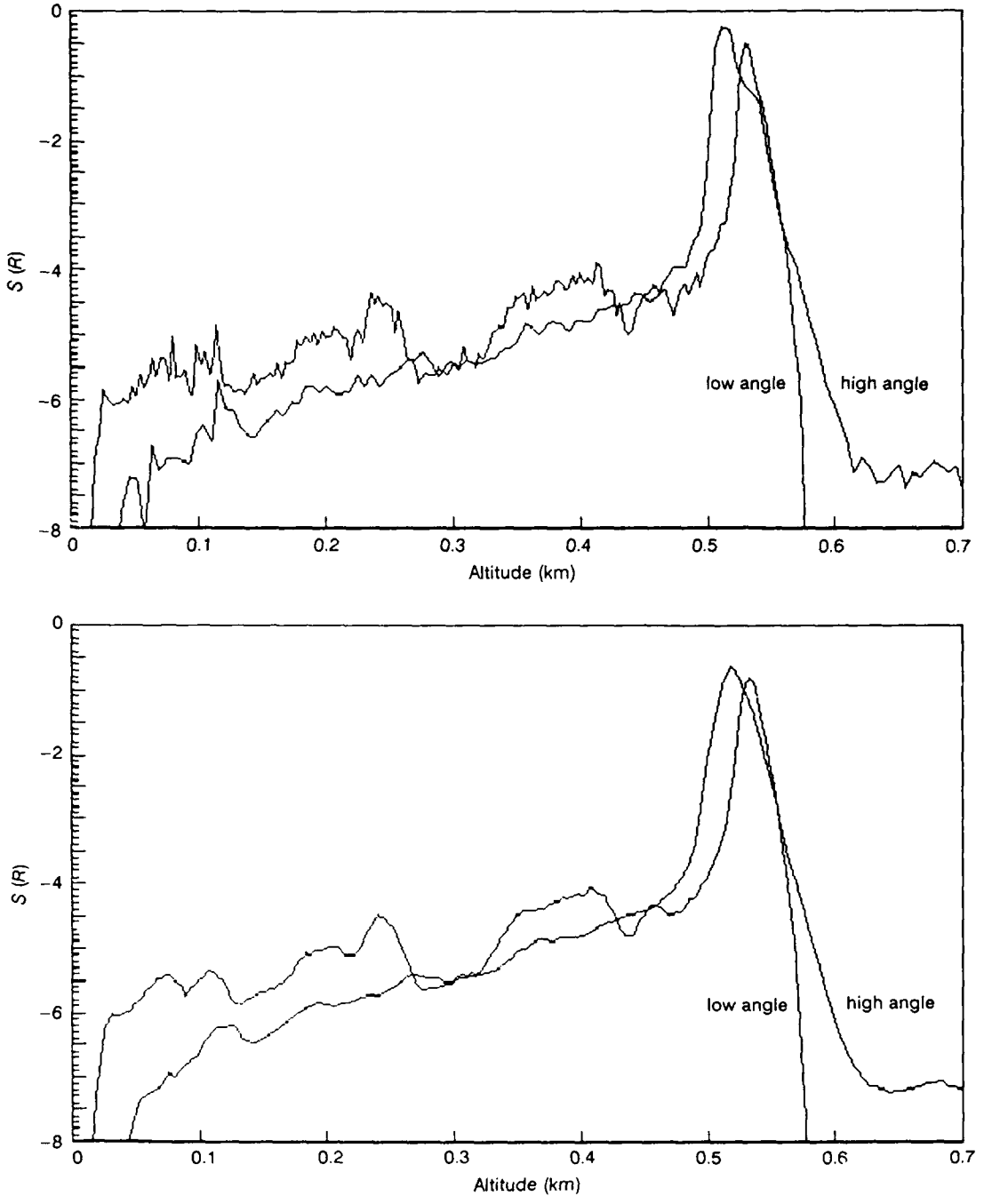

Figure 3. An example of two-elevation-angle lidar shots made on 17 May 1989. Upper graph is for no averaging and lower graph is for a 5-point running average.

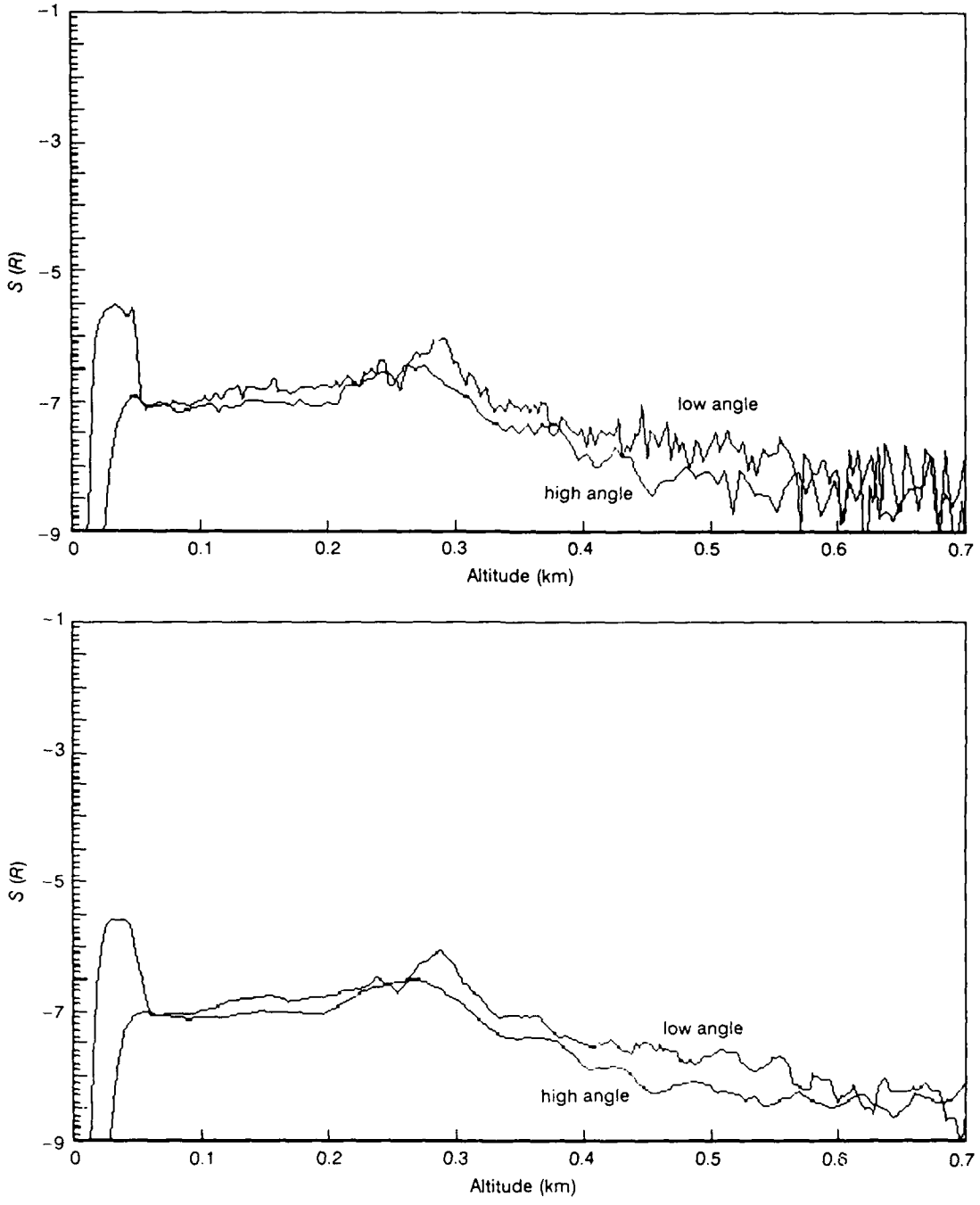

Figure 4. An example of two-elevation-angle lidar shots made on 24 May 1989. Upper graph is for no averaging and lower graph is for a 5-point running average.

DATA ANALYSIS AND RESULTS

After a 5-point running average was calculated for each lidar return, Eq. 9 was applied to these data to get a nominal integrated extinction, or optical depth. An upper altitude, or h_2, of 475 meters was used for data set 9, taken on May 17. An altitude of 500 meters was used for data sets 11 and 12 on May 17 and for data sets 8 and 14 on May 24.

Lower altitude, or h_1, values from 100 to about 400 meters in 25-meter increments were used in Eq. 9 to calculate optical depth. These optical depth calculations are listed in Table 1 for May 17 and in Table 2 for May 24. The argument here is that, if the atmosphere is horizontally homogenous, the optical depth should consistently decrease as h_1 increases and the vertical path decreases. As can be seen from Tables 1 and 2, this is not the case. For data set 9 the optical depth from 275 to 475 meters, or a 200-meter path, is 0.15 while that from 375 to 475 meters, or a 100-meter path, is 0.49. Similar results occur for data set 11 and data set 12. For data sets 8 and 14 taken on May 24 many of the optical depth values are negative.

Horizontal inhomogeneities are also evident in the various plots of $S(R)$ versus altitude found in the Appendix, as well as those shown in Fig. 3 and 4. These inhomogeneities show up as differences in the structure on the two traces.

Table 1. Optical depth calculations made for different height interva ; for data taken on 17 May 1989.

Data Set 9*	
Lower Altitude (m)	Optical Depth
100	0.811
125	0.437
150	0.584
175	0.597
200	0.647
225	0.584
250	0.688
275	0.150
300	0.260
325	0.260
350	0.342
375	0.494

*Upper Altitude 475 meters

(Contd)

Table 1. Contd.

Data Set 11*	
Lower Altitude (m)	Optical Depth
100	0.036
125	0.136
150	0.119
175	0.289
200	0.395
225	0.256
250	0.223
275	0.277
300	0.262
325	0.262
350	0.128
375	0.068
400	0.116

*Upper Altitude 500 meters

Data Set 12*	
Lower Altitude (m)	Optical Depth
100	0.263
125	0.066
150	0.420
175	0.823
200	0.906
225	0.526
250	0.528
275	0.299
300	0.211
325	0.363
350	0.256
375	0.418
400	0.382

*Upper Altitude 500 meters

Table 2. Optical depth calculations made for different height intervals for data taken on 24 May 1989.

Data Set 8*	
Lower Altitude (m)	Optical Depth
100	-0.150
125	-0.085
150	-0.093
175	-0.116
200	-0.084
225	-0.170
250	-0.260
275	-0.054
300	-0.035
325	0.059
350	0.025
375	0.137
400	-0.023

*Upper Altitude 500 meters

Data Set 14*	
Lower Altitude (m)	Optical Depth
100	0.019
125	0.047
150	-0.014
175	0.014
200	-0.026
225	0.055
250	0.035
275	0.031
300	0.194
325	0.018
350	0.027
375	0.017
400	0.114

*Upper Altitude 500 meters

CONCLUSIONS

Lidar measurements made at two elevation angles cannot be used to determine vertical integrated extinction, or optical depth, with any degree of accuracy. The atmospheric conditions are not sufficiently horizontally homogeneous for this method to work. This horizontal homogeneity is a requirement of the theory.

REFERENCES

Klett, J.D., "Stable analytical inversion solution for processing lidar returns," Appl. Opt. 20, 211 (1981).

Klett, J.D., "Lidar inversion with variable backscatter extinction ratios," Appl. Opt. 24, 1638 (1985).

Kunz, G.J., "A method for measuring the vertical extinction and backscatter profile with a scanning lidar," TNO Physics and Electronics Laboratory, The Hague, The Netherlands, FEL 1988-65 (1988).

Lentz, W.J., "The visioceilometer: a portable visibility and cloud ceiling height lidar," Atmospheric Sciences Laboratory, White Sands, New Mexico, TR-0105 (1982).

Paulson, M.R., "Lidar measurements indicating atmospheric inhomogeneities," Naval Ocean System Center, San Diego, Calif., TD 867 (1986).

Russell, P.B., and J.M. Livingston, "Slant-path extinction measurements and their relation to measured and calculated albedo changes," J. Clim. and Appl. Meteor. 23, 1204 (1984).

Spinhirne, J.D., J.A. Reagan, and B.M. Herman, "Vertical distribution of aerosol extinction cross section and inference of aerosol imaginary index in the troposphere by lidar technique," J. Appl. Meteor. 19, 426 (1980).

Appendix

GRAPHS OF $S(R)$ VERSUS ALTITUDE FOR 17 MAY 1989 AND 24 MAY 1989

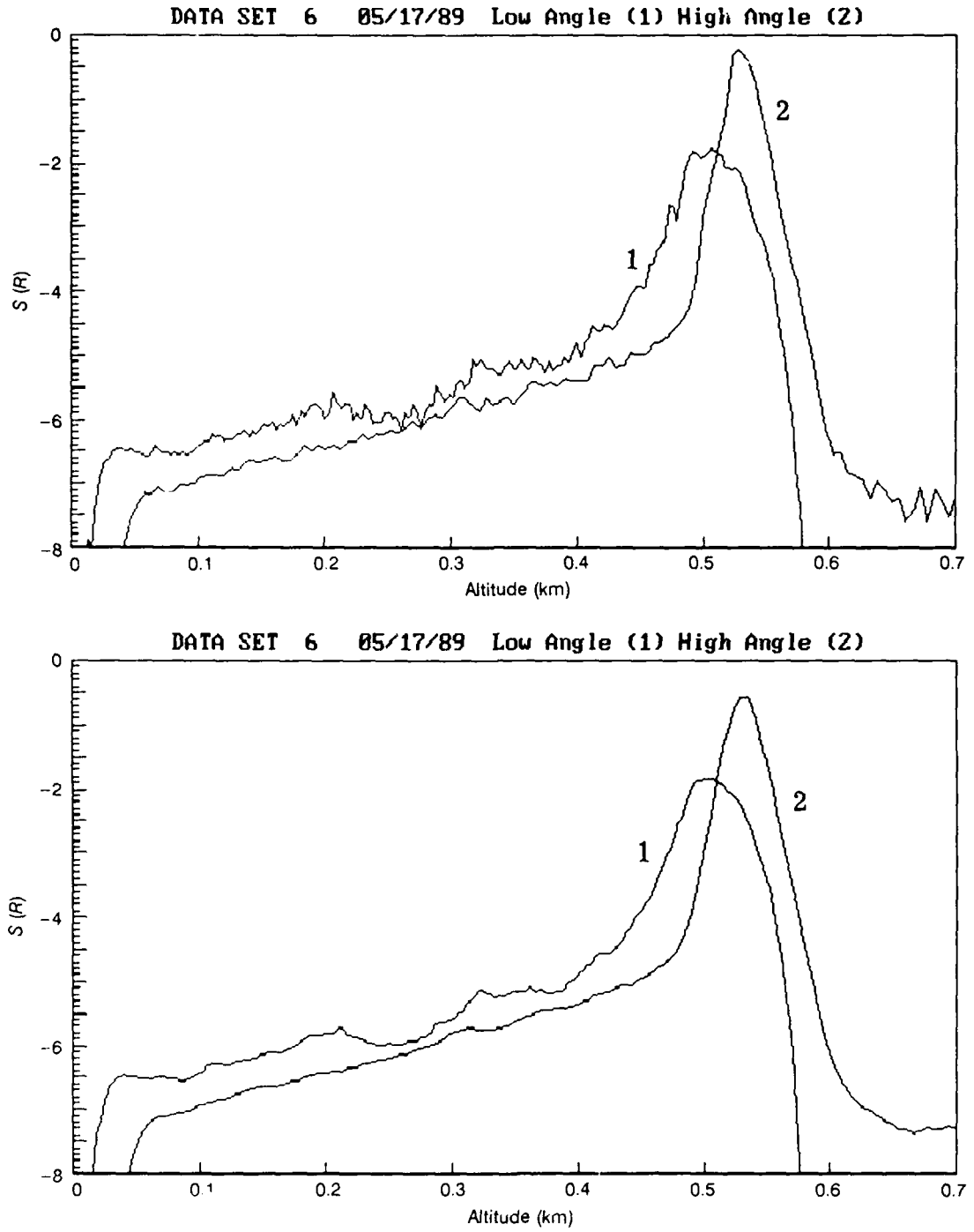

Figure A-1. *S* (*R*) versus altitude for data set 6 through 9 and 11 through 15 taken on 17 May 1989 and data set 7 through 15 taken on 24 May 1989. The two elevation angles were 15 degrees and 50 degrees. Upper graph is unsmoothed data and lower graph is a 5-point running average.

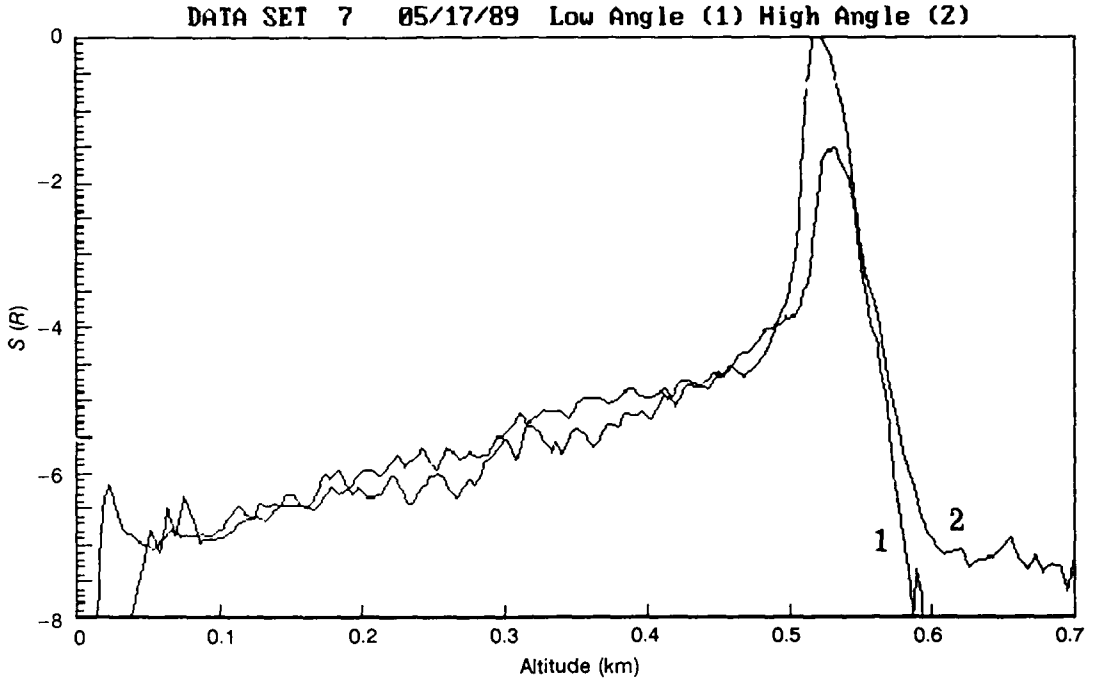

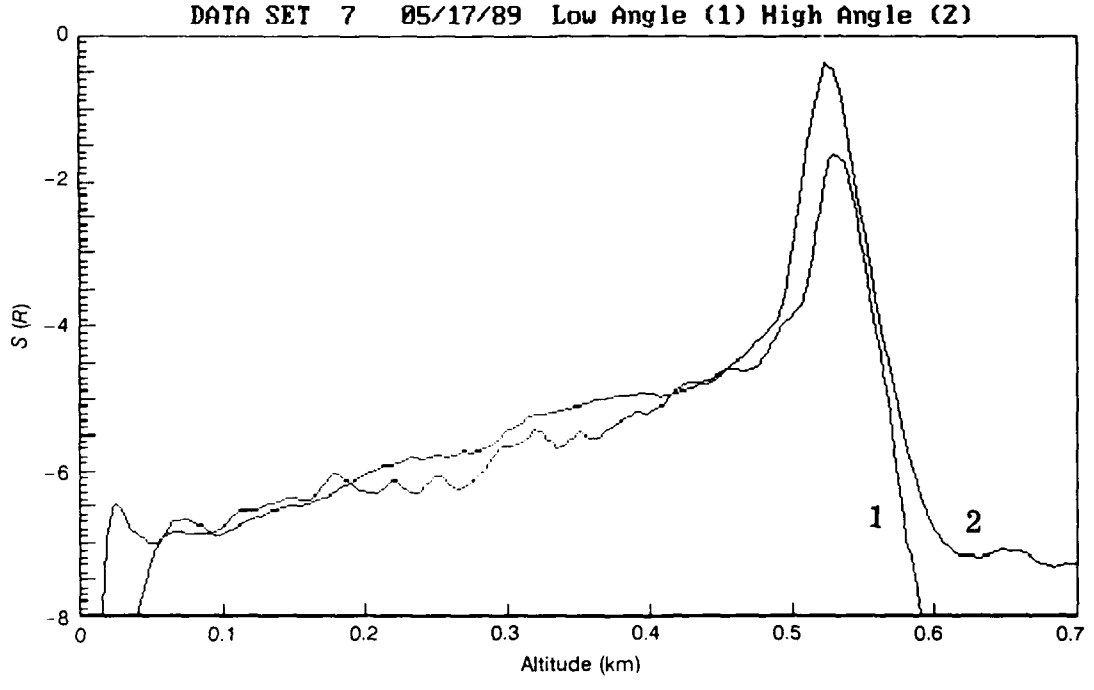

Figure A-1. Contd.

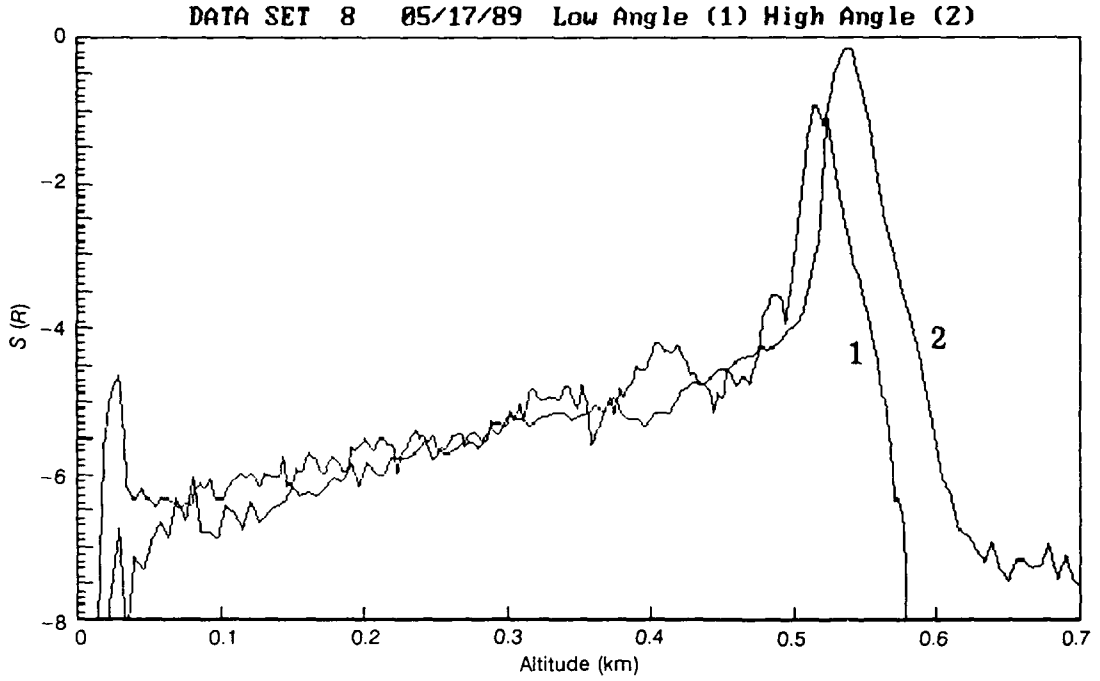

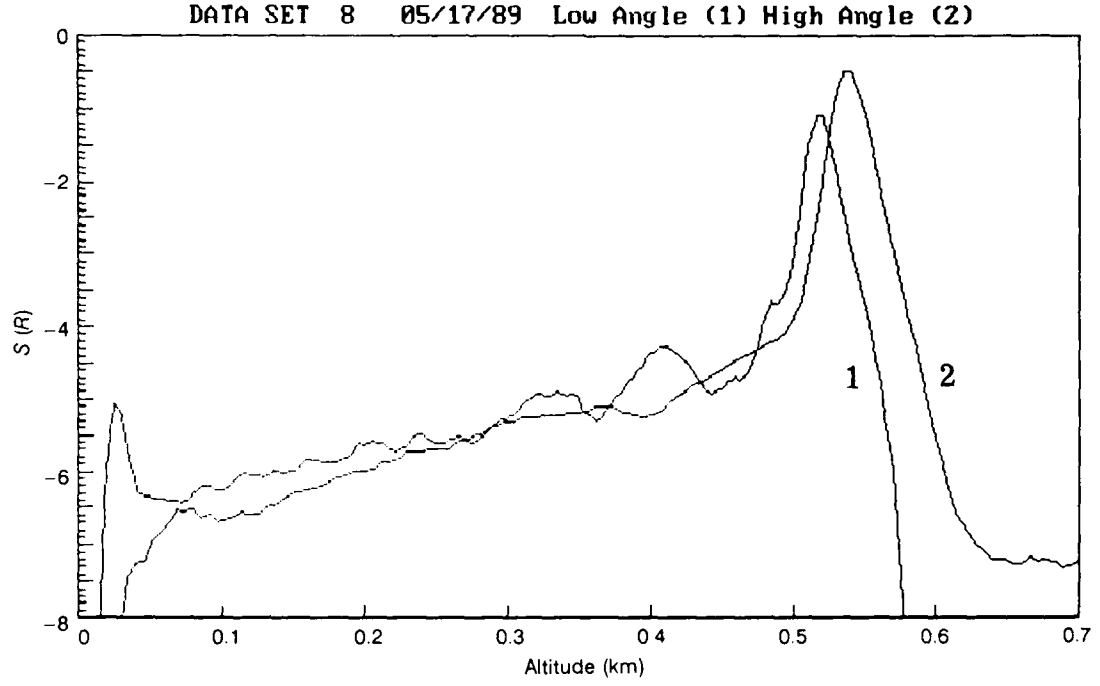

Figure A-1. Contd.

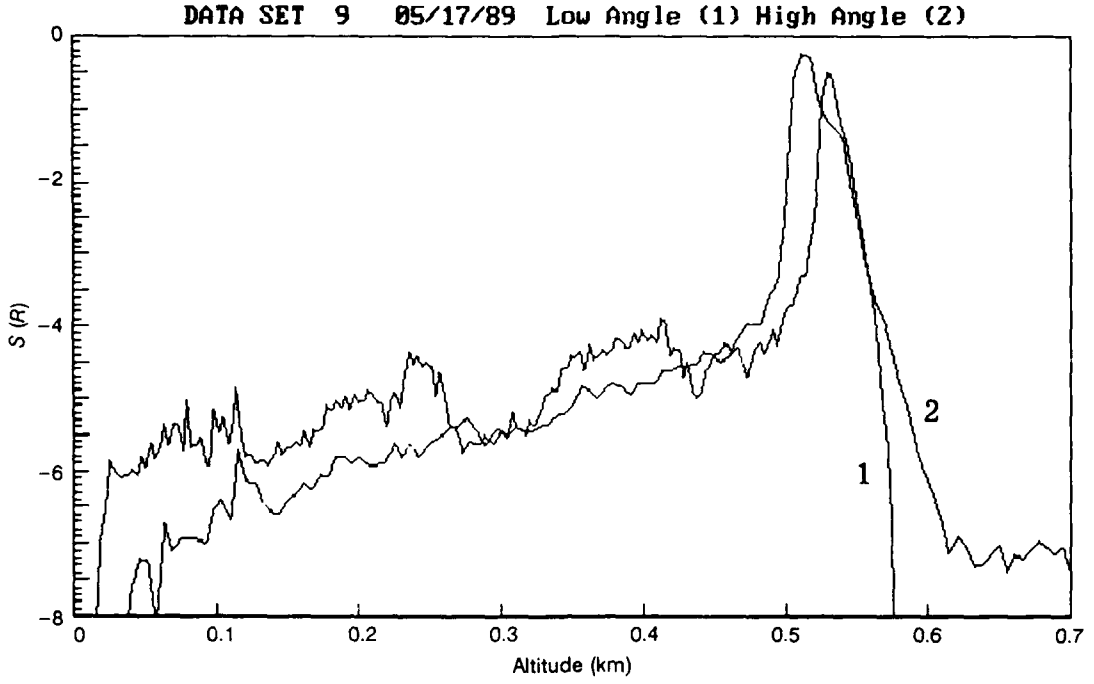

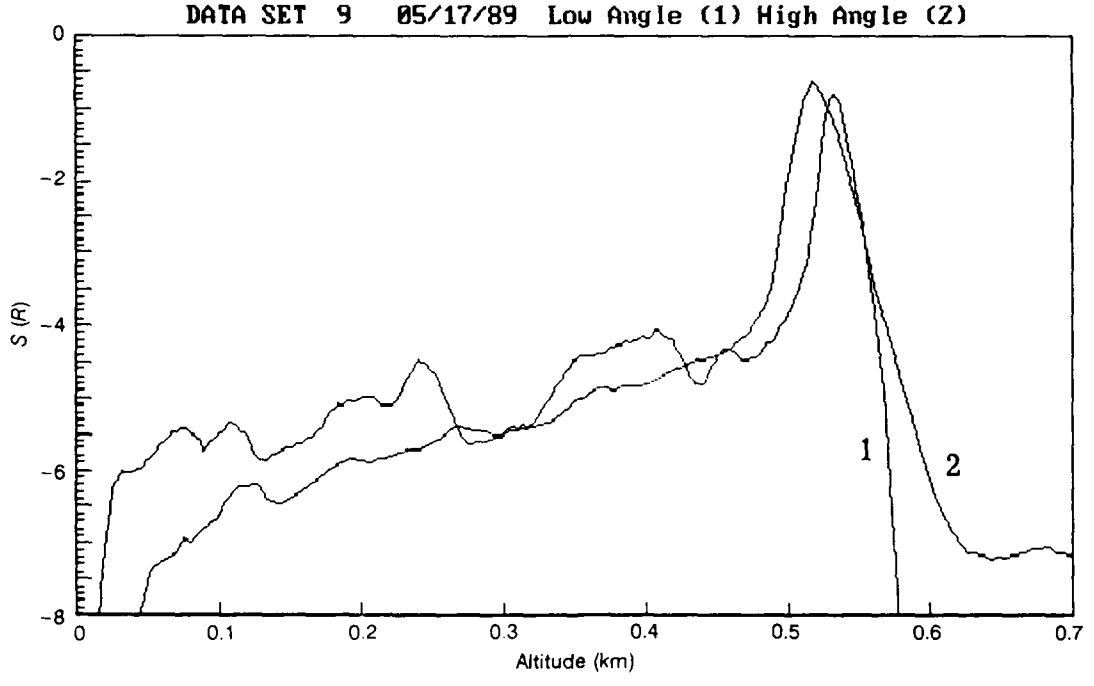

Figure A-1. Contd.

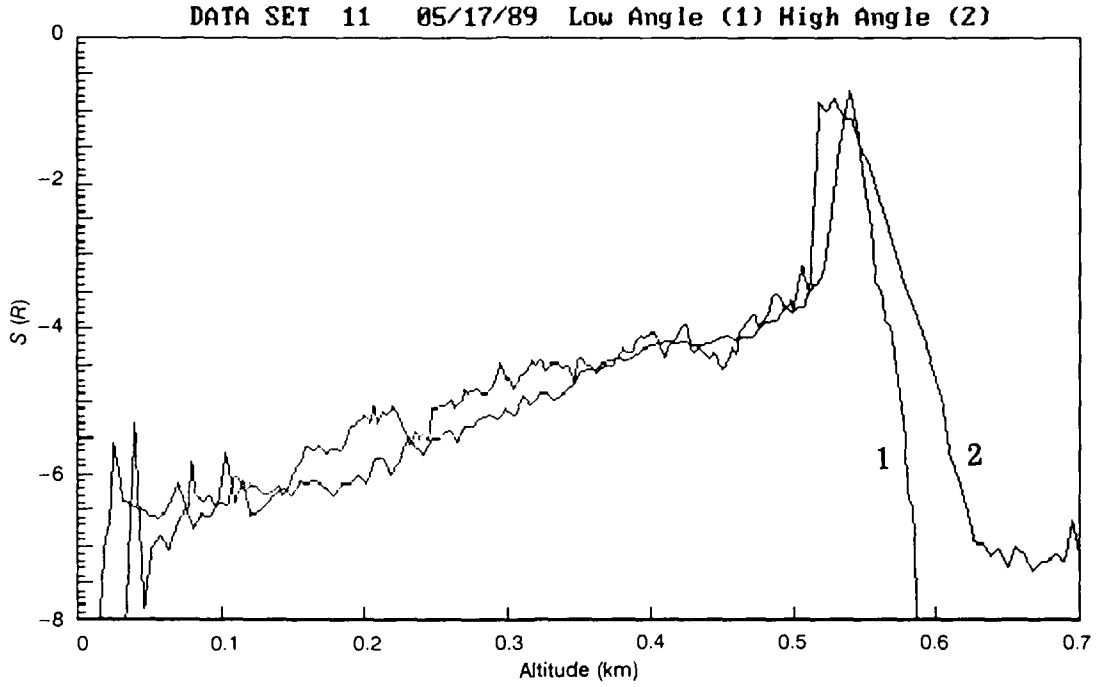

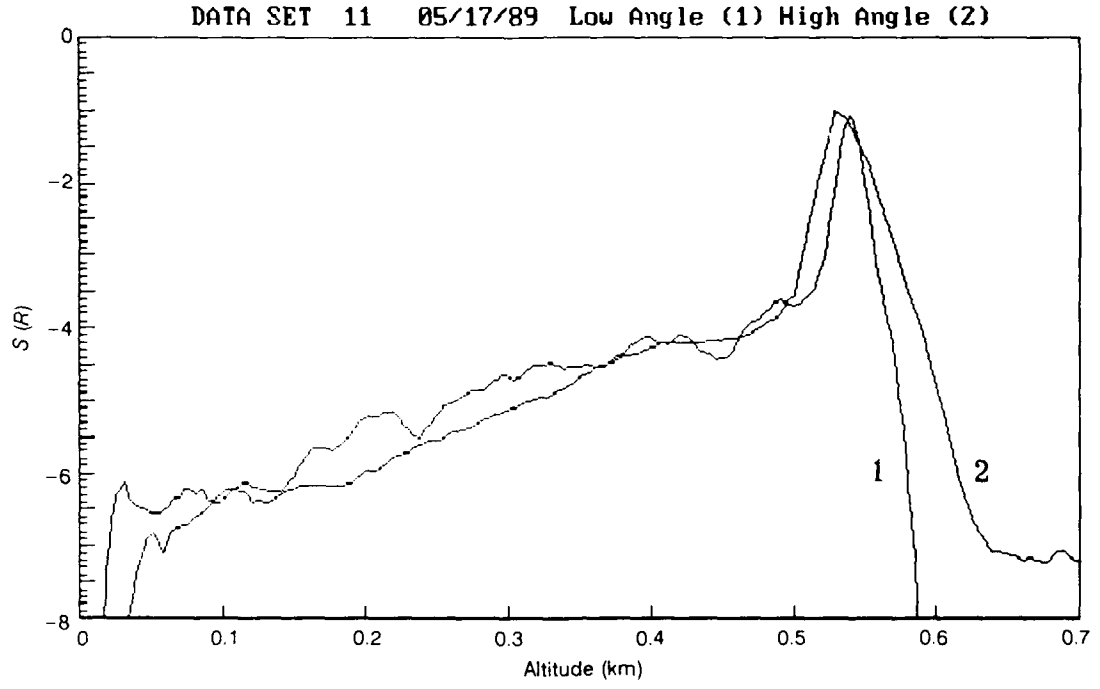

Figure A-1. Contd.

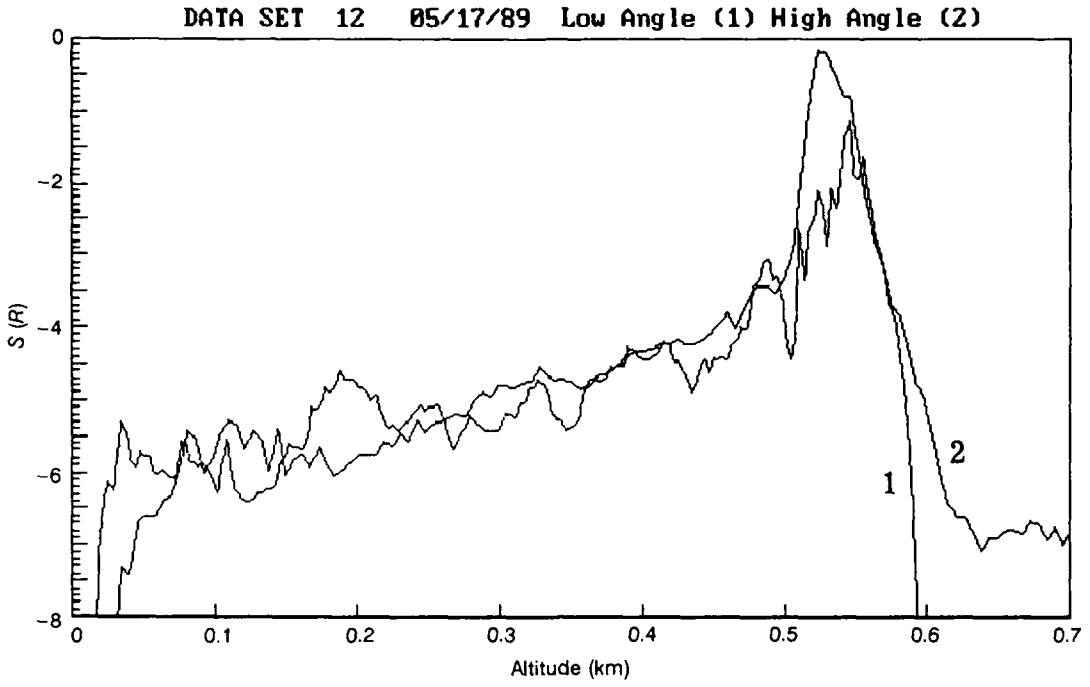

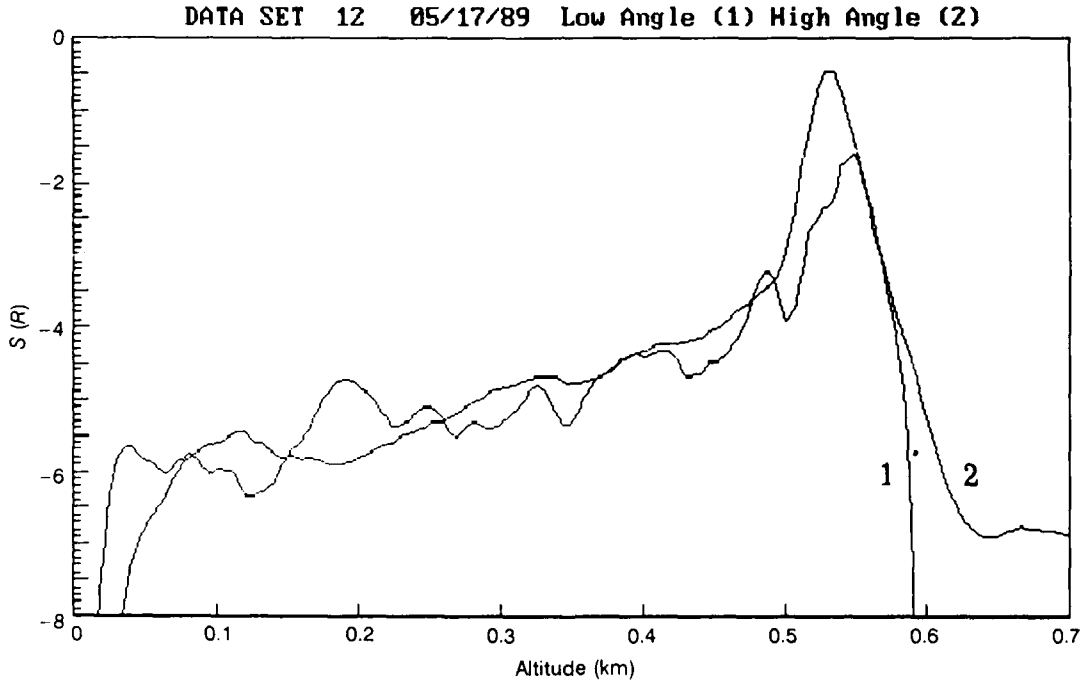

Figure A-1. Contd.

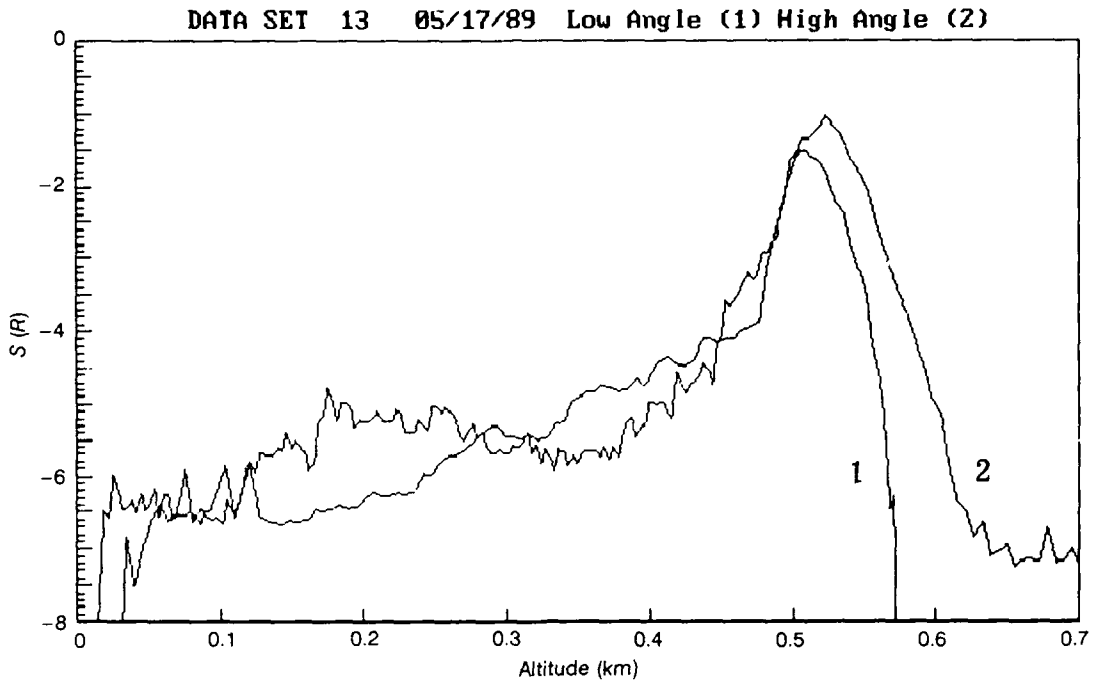

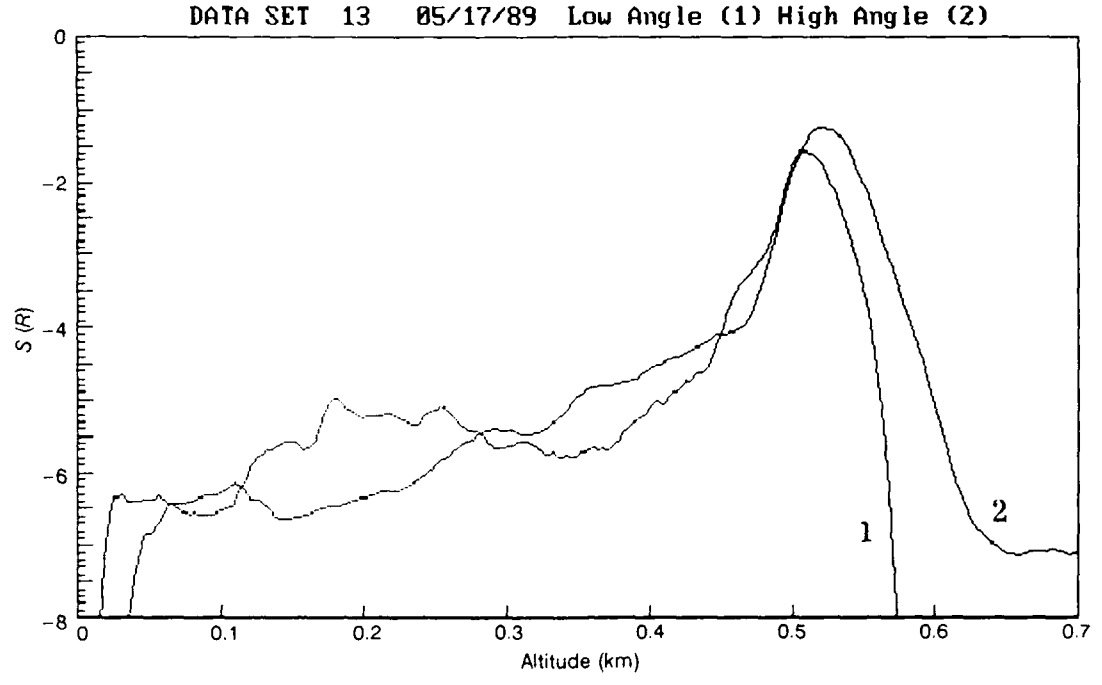

Figure A-1. Contd.

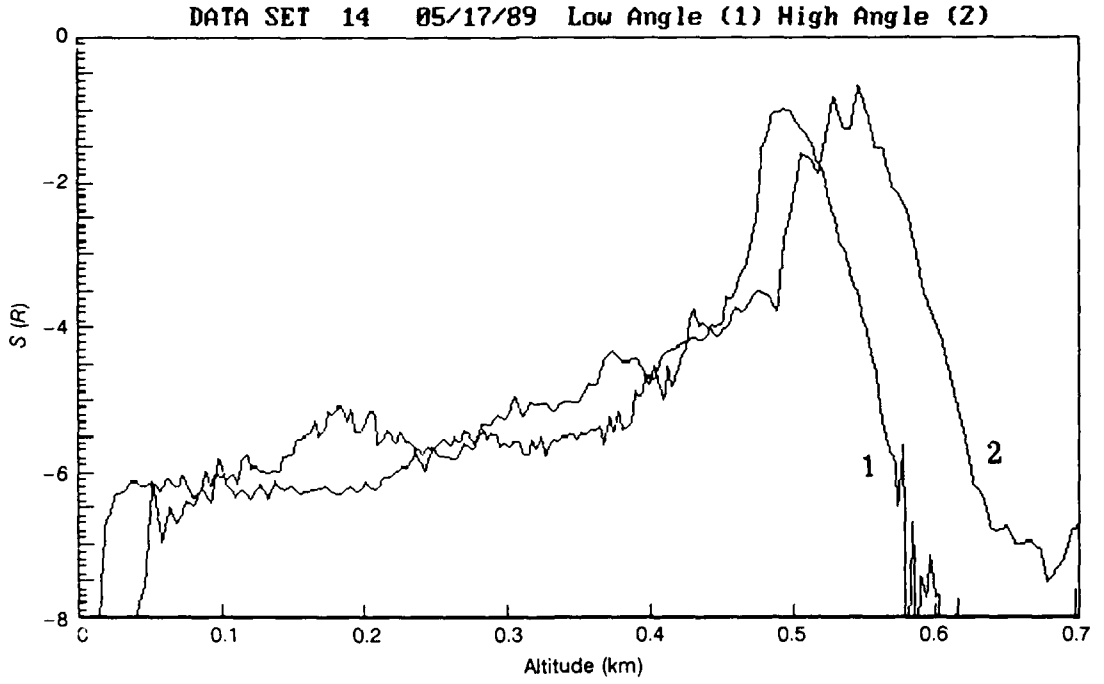

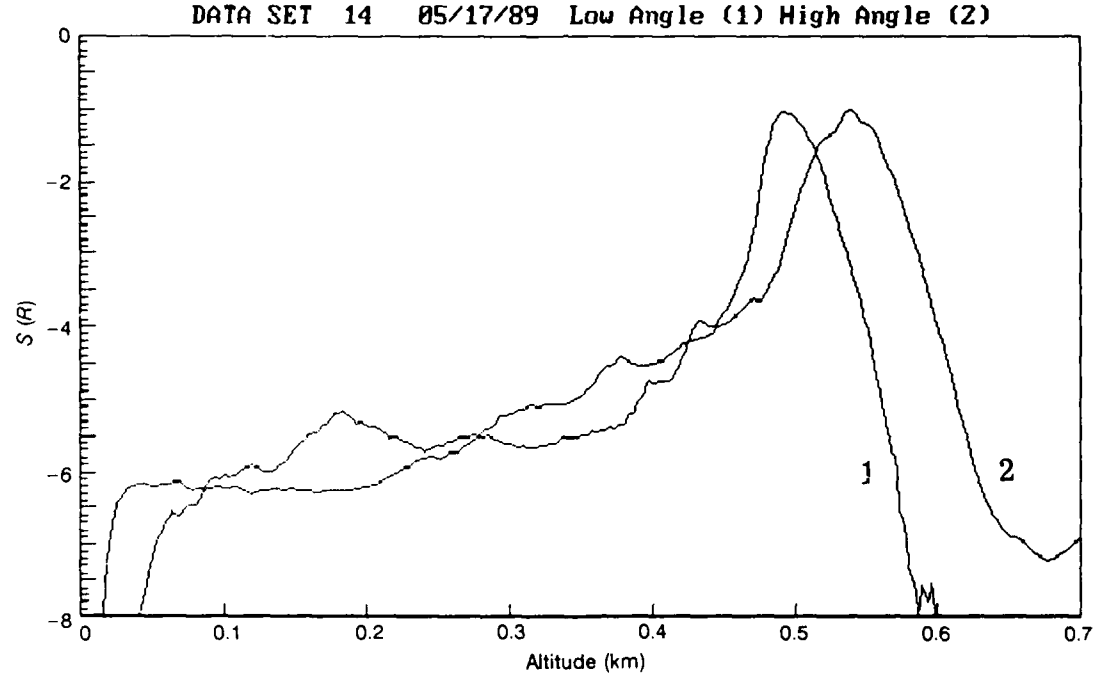

Figure A-1. Contd.

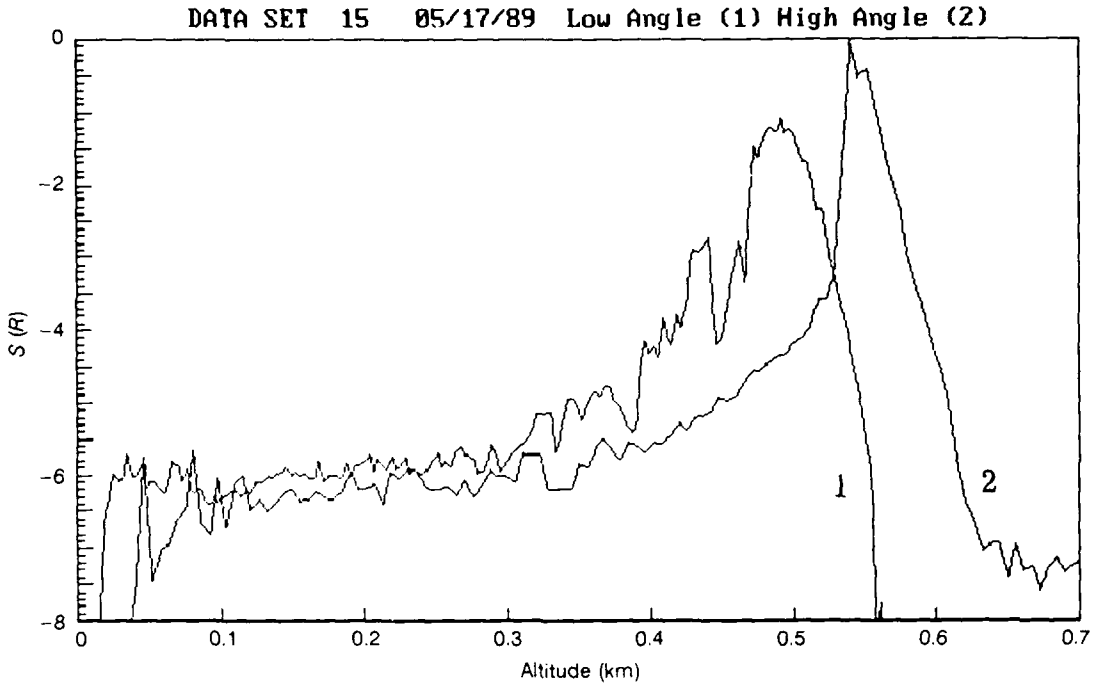

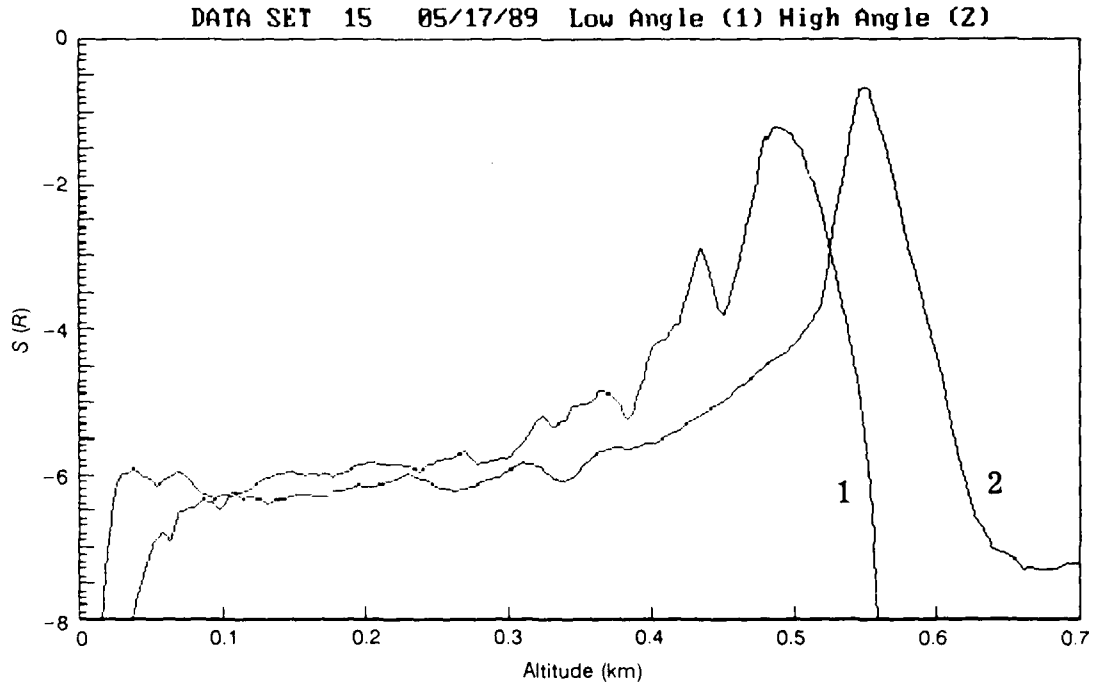

Figure A-1. Contd.

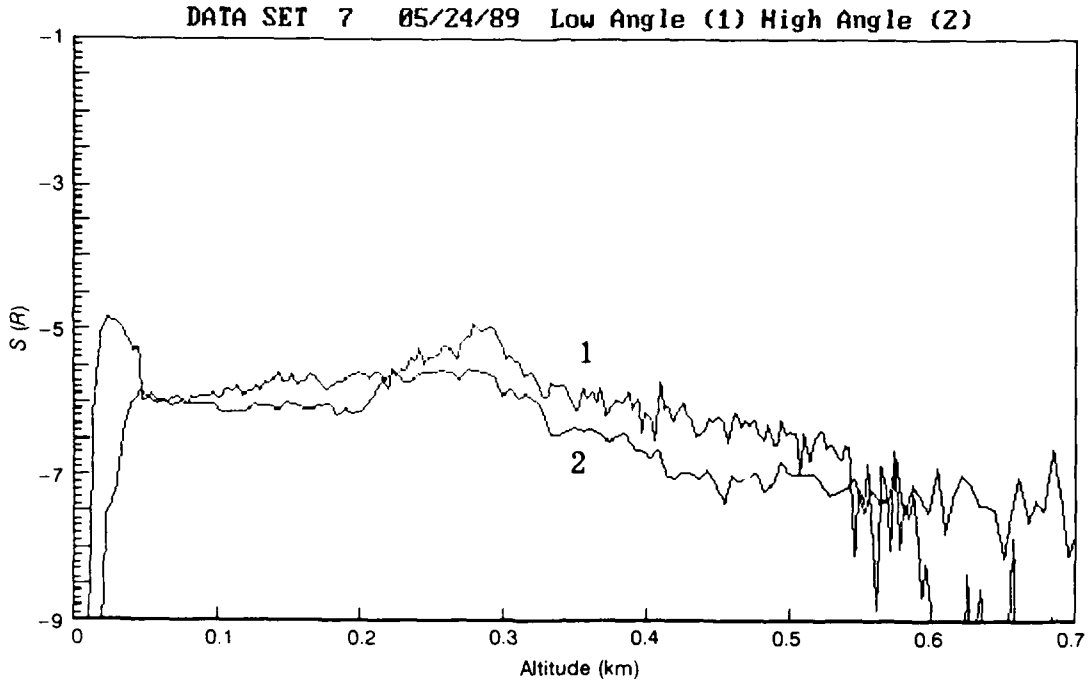

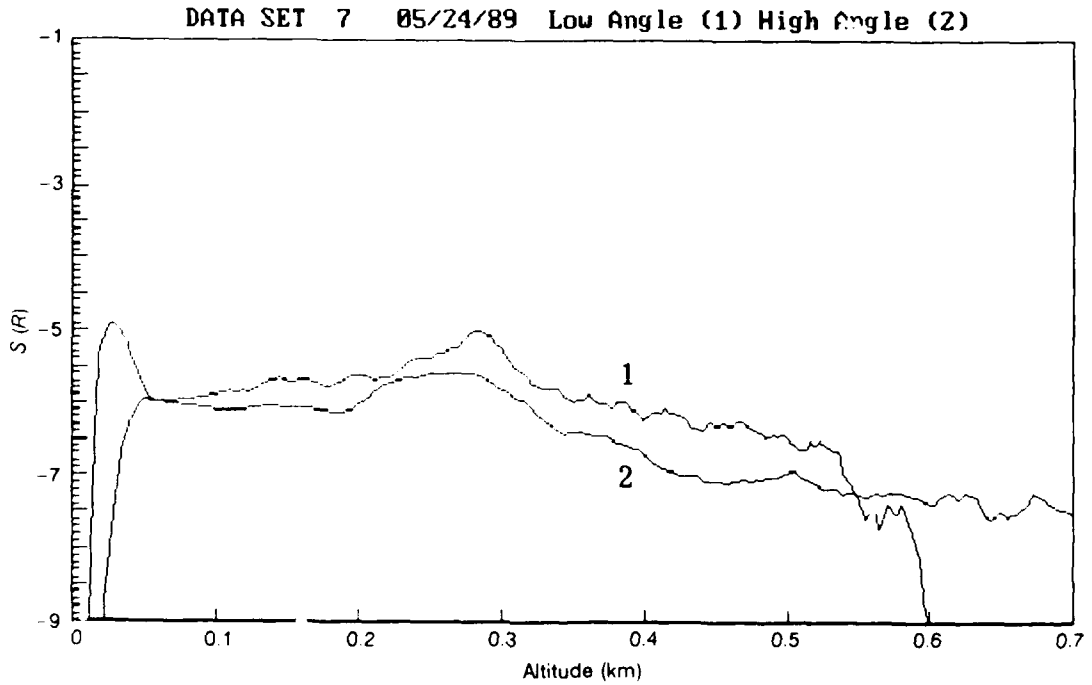

Figure A-1. Contd.

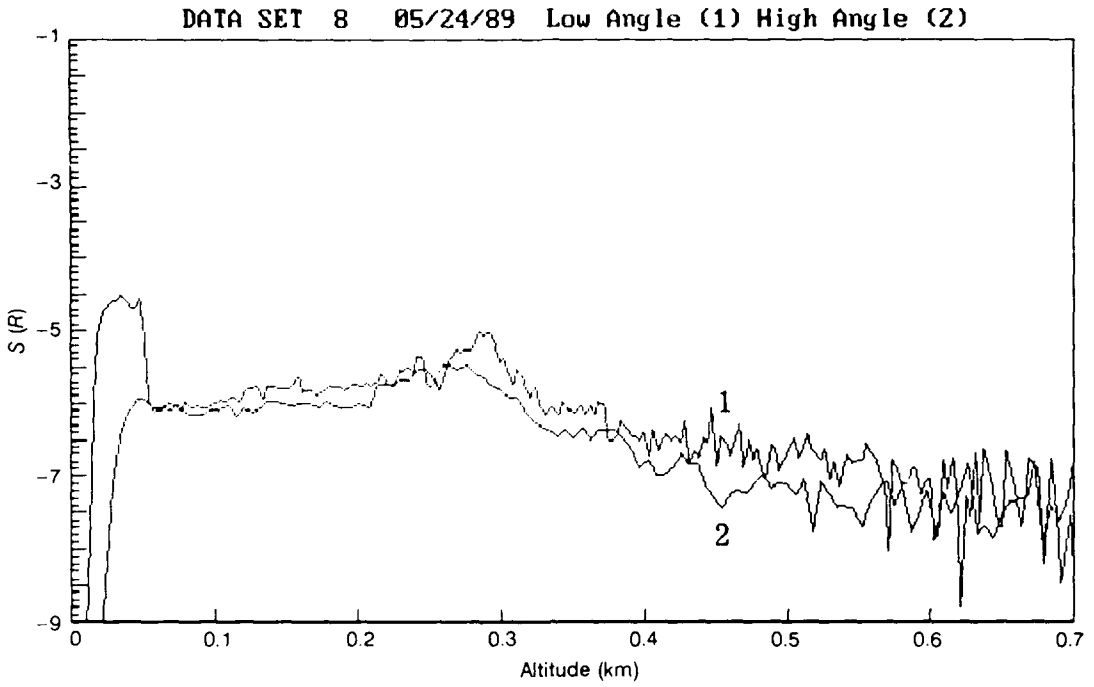

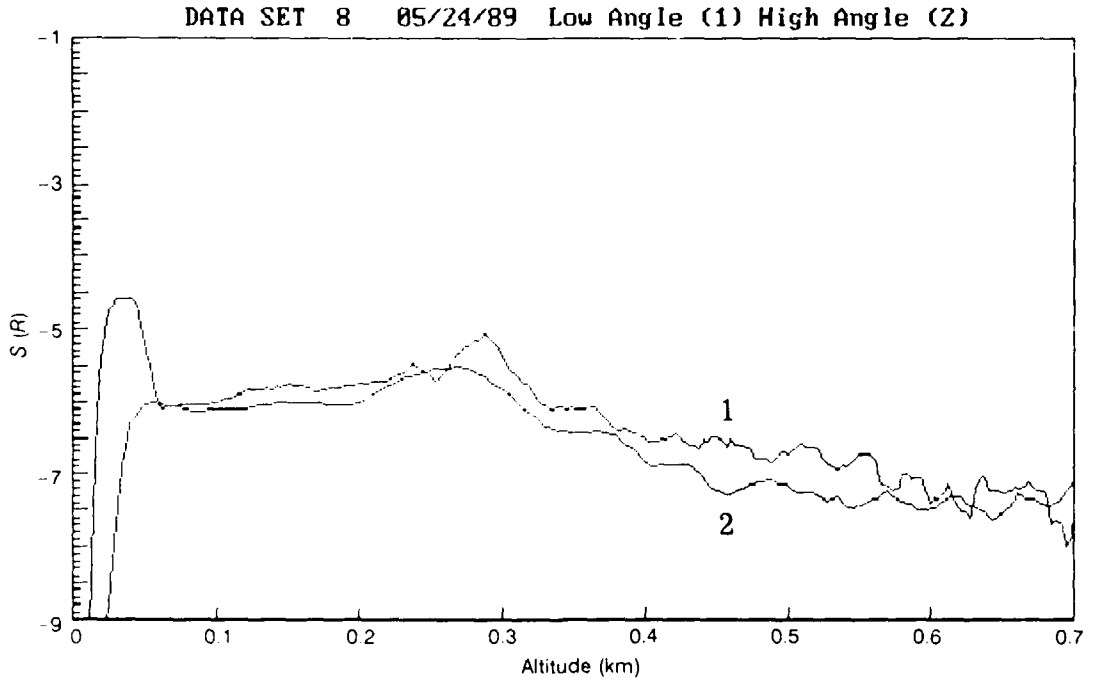

Figure A-1. Contd.

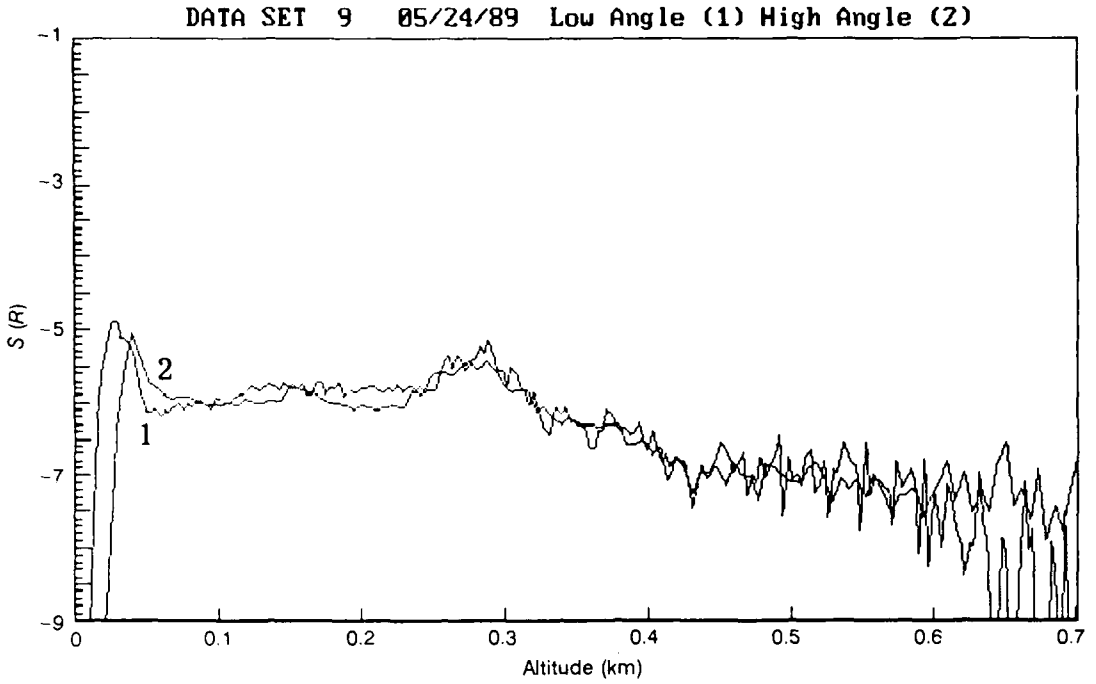

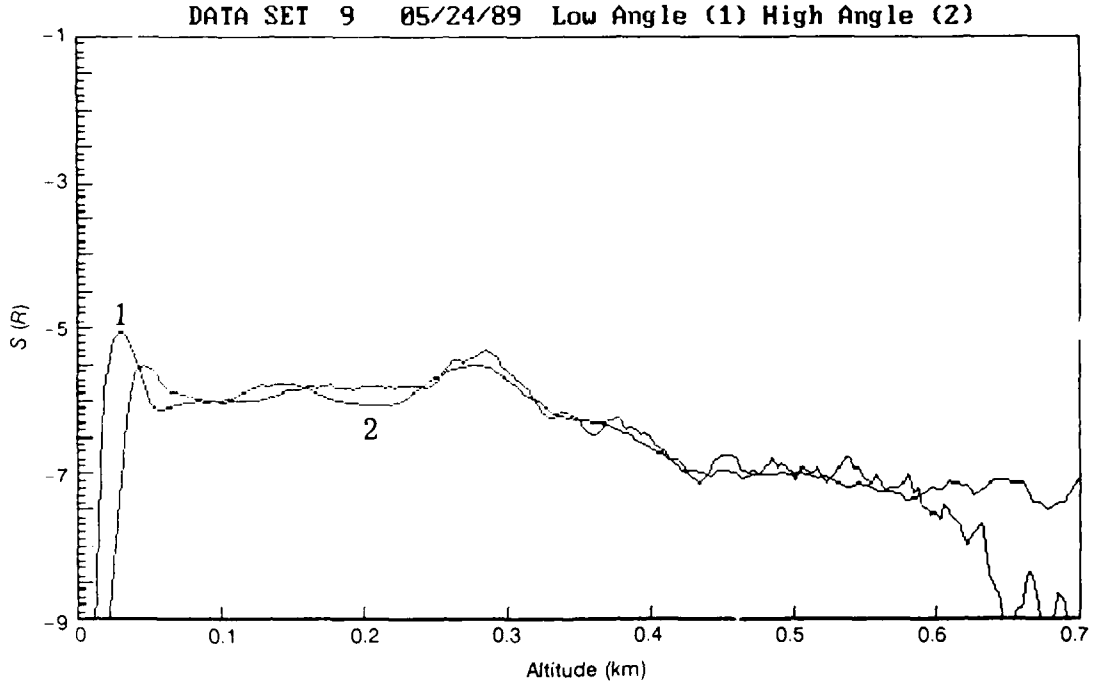

Figure A-1. Contd.

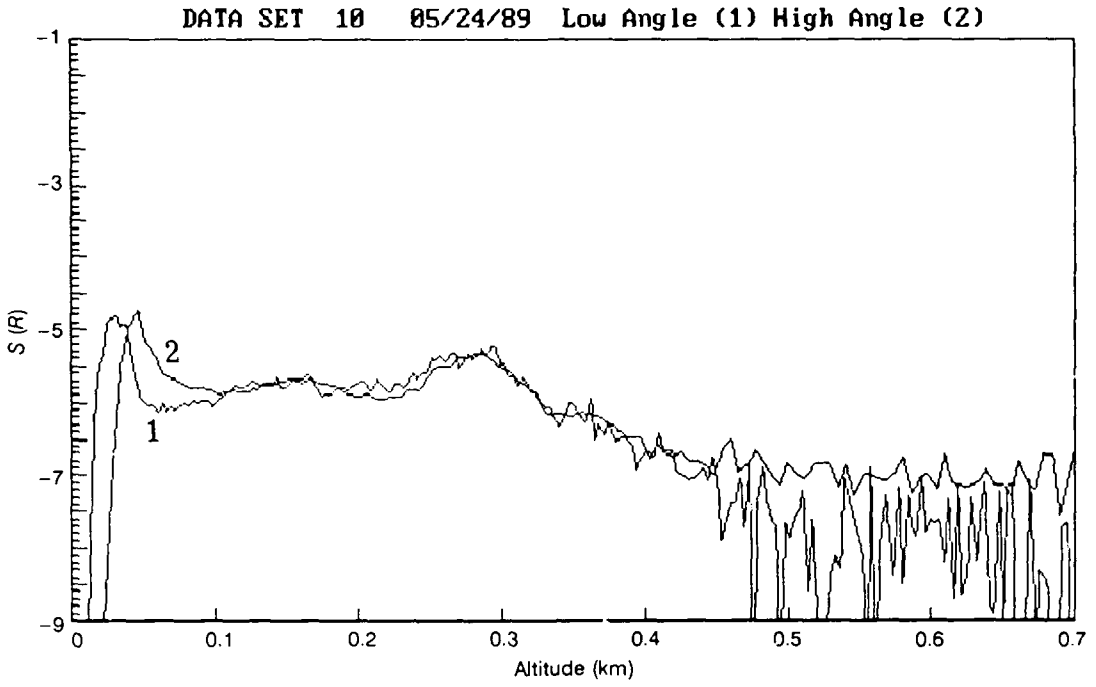

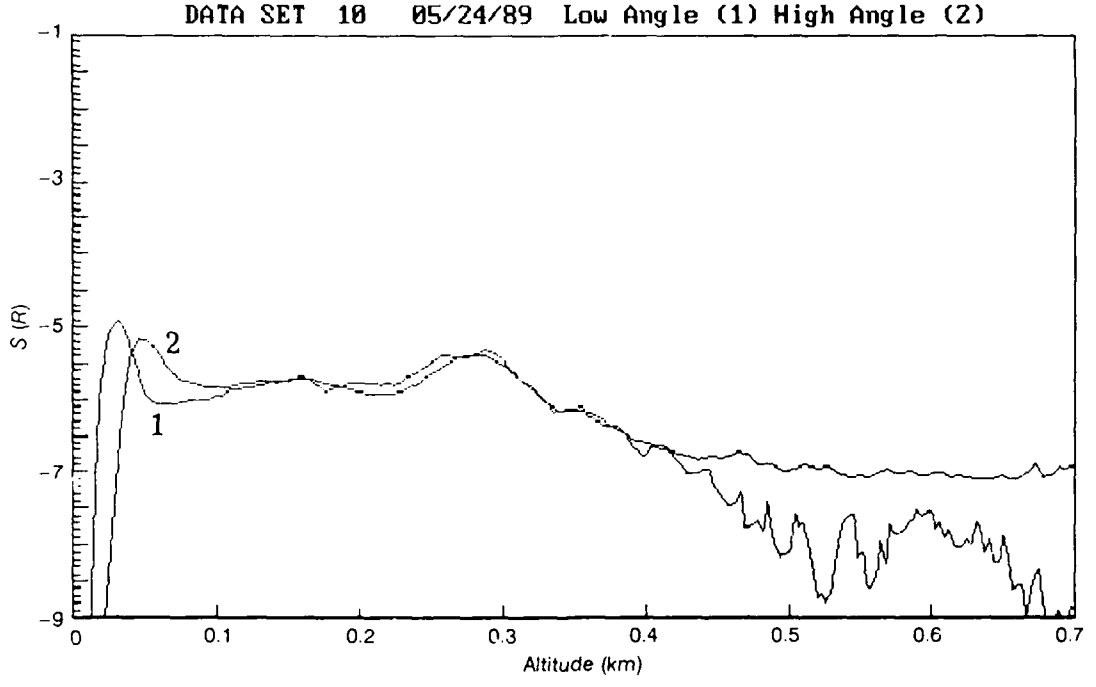

Figure A-1. Contd.

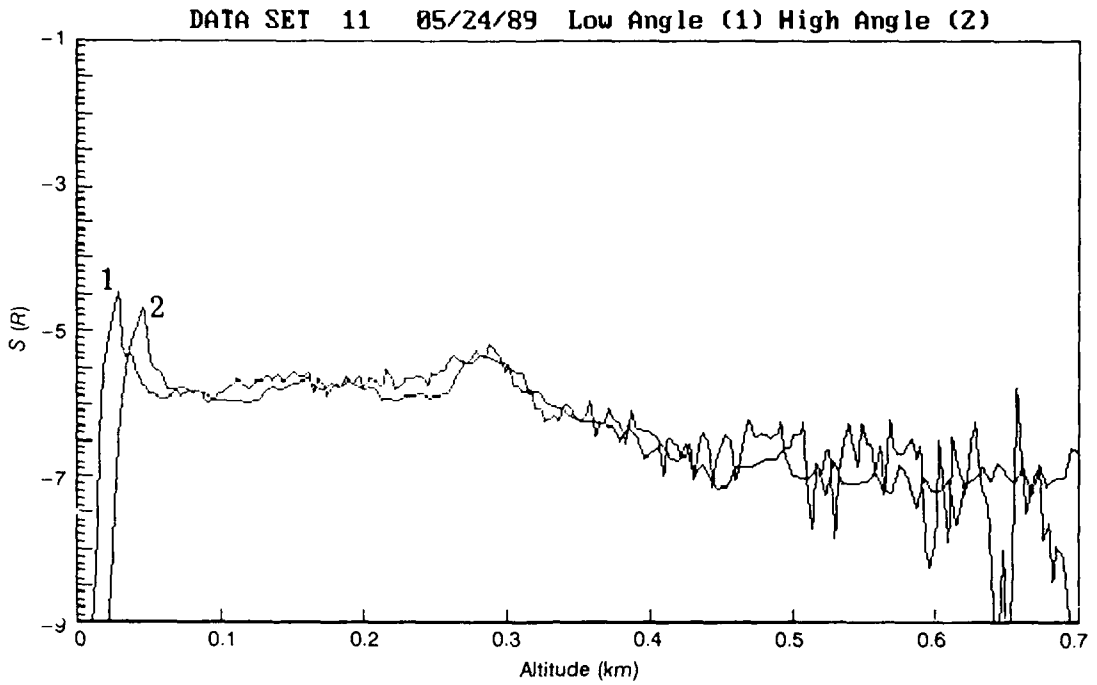

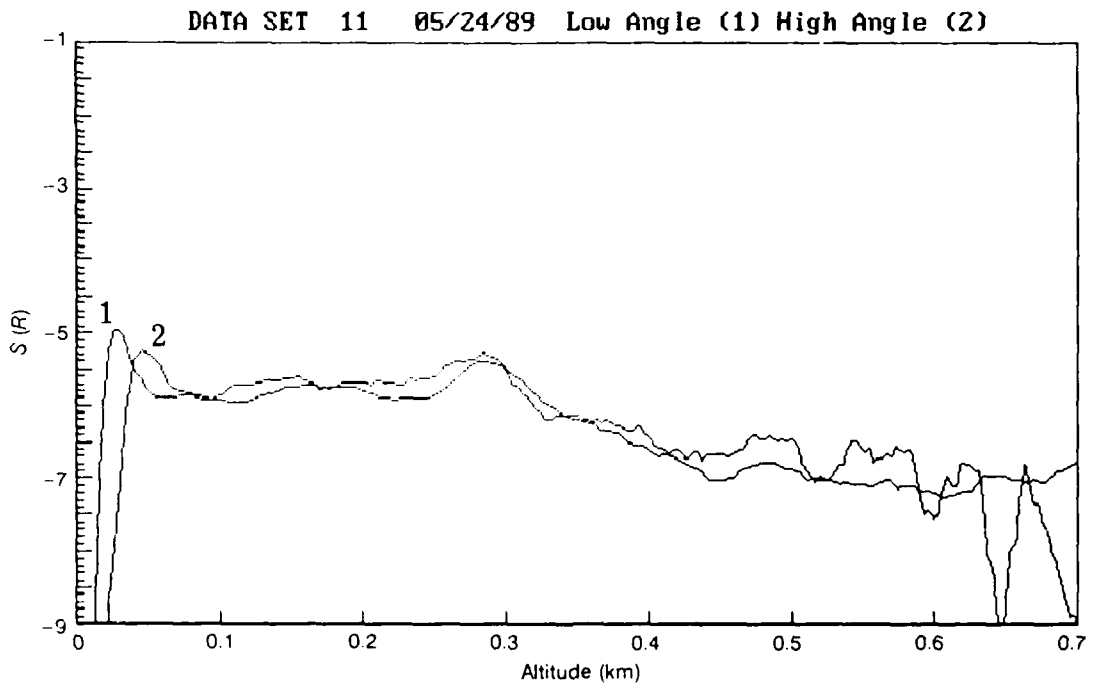

Figure A-1. Contd.

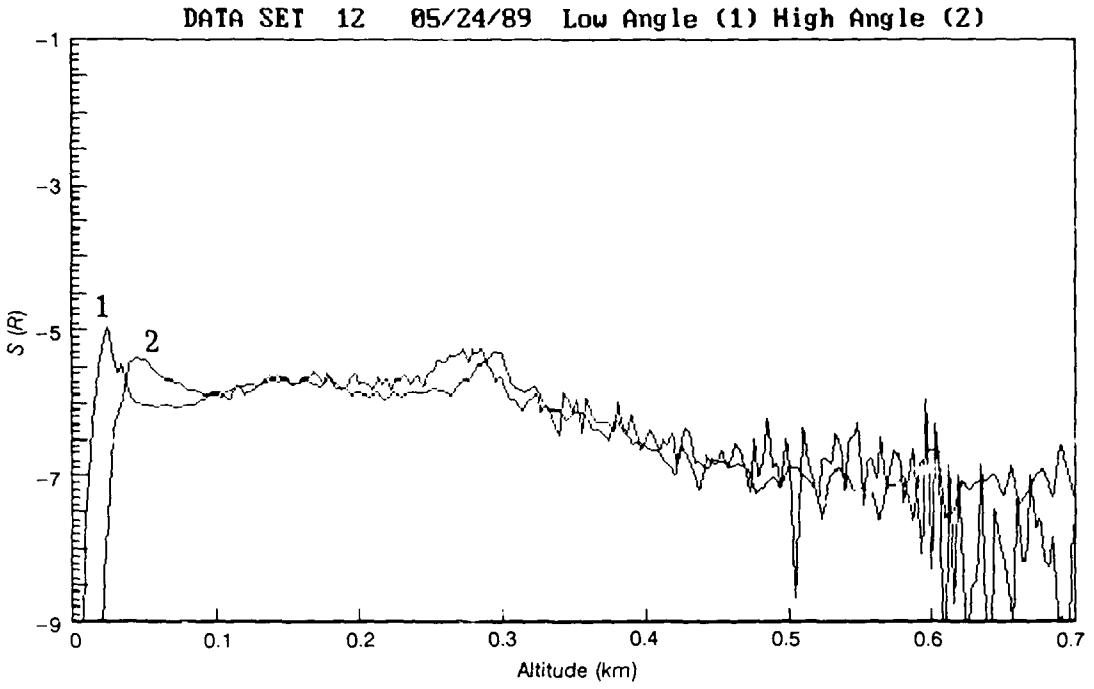

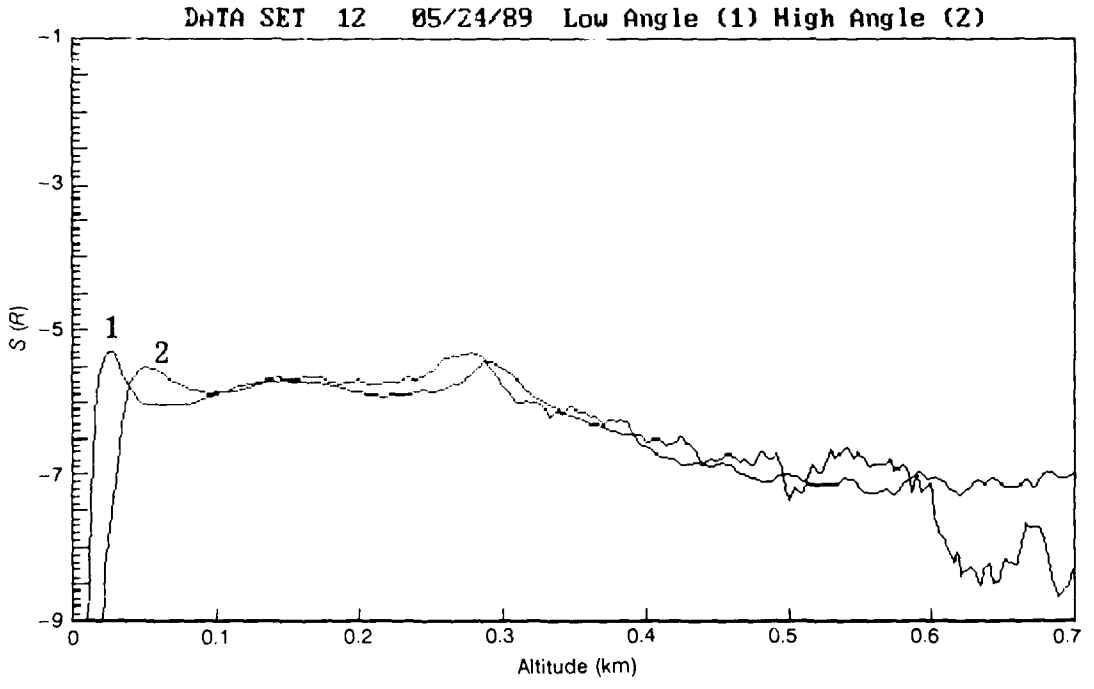

Figure A-1. Contd.

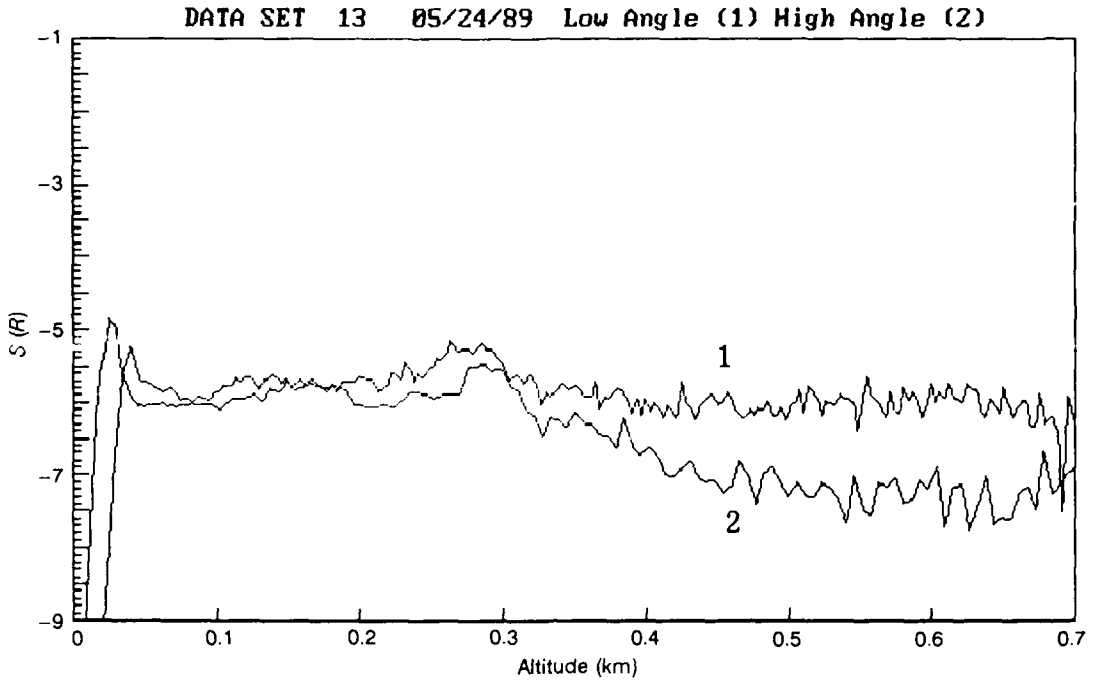

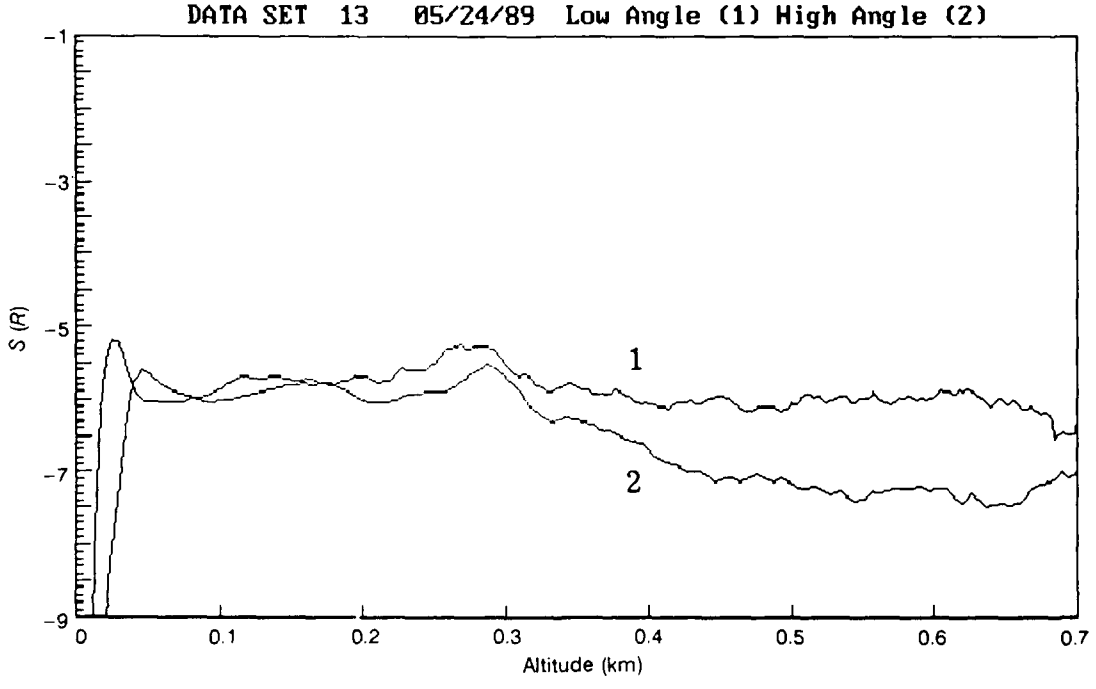

Figure A-1. Contd.

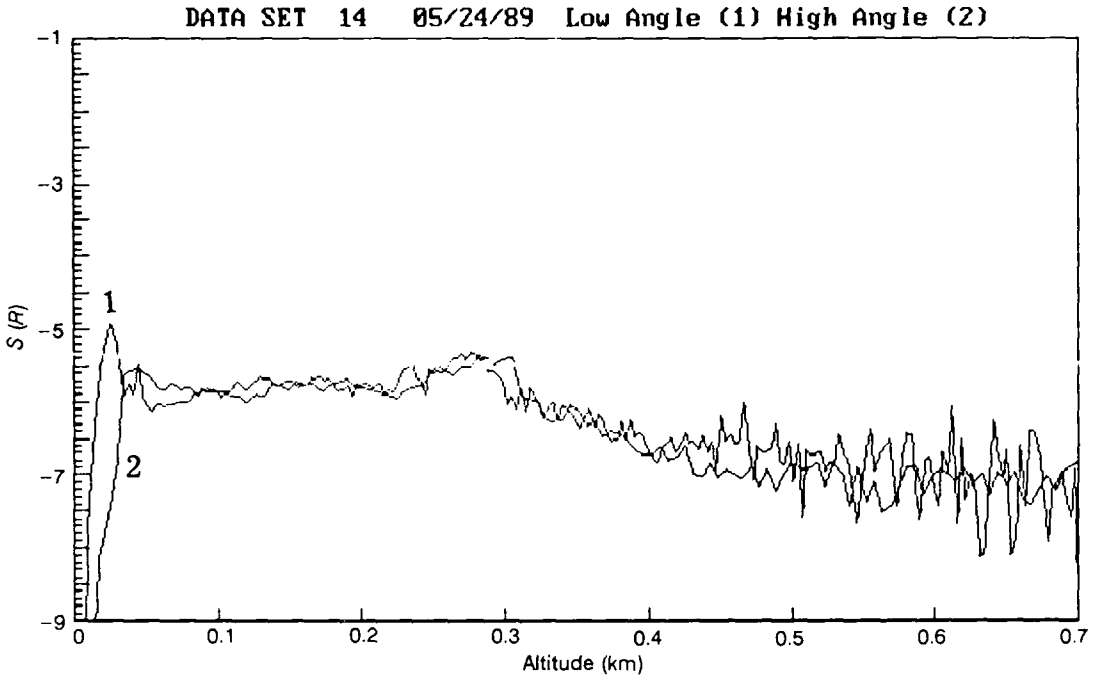

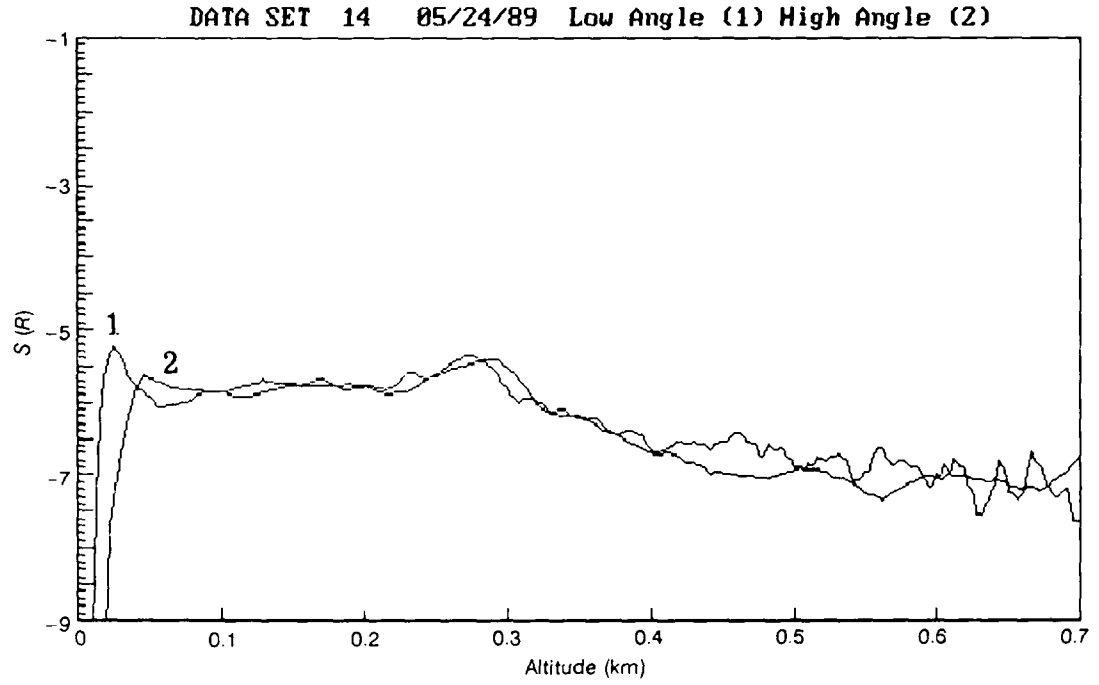

Figure A-1. Contd.

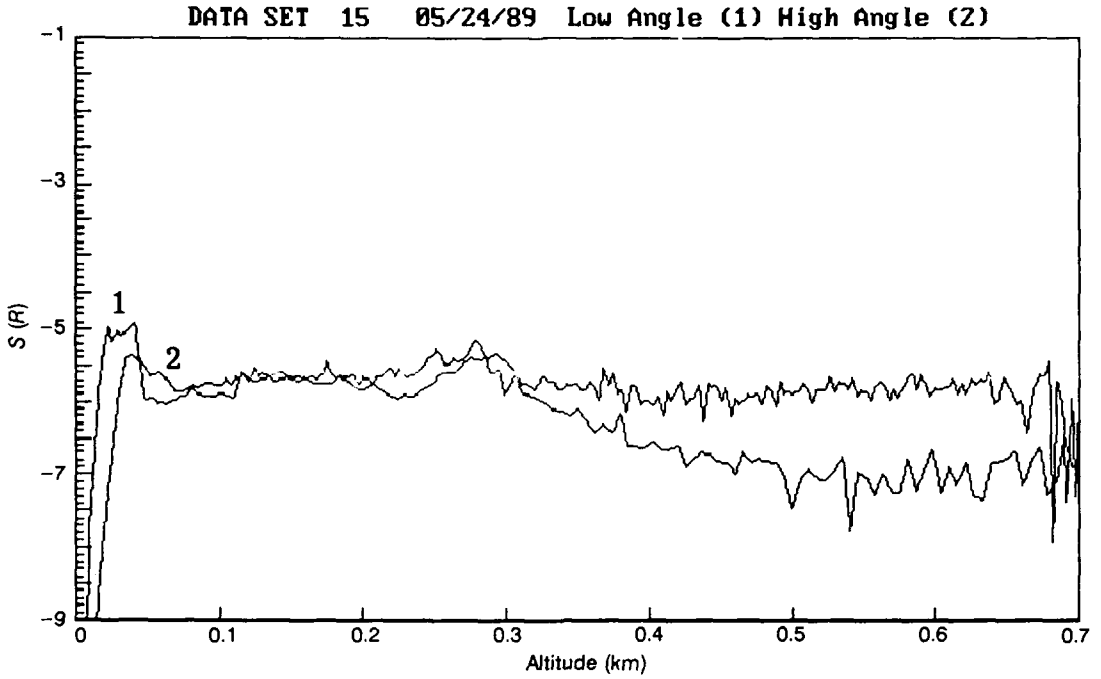

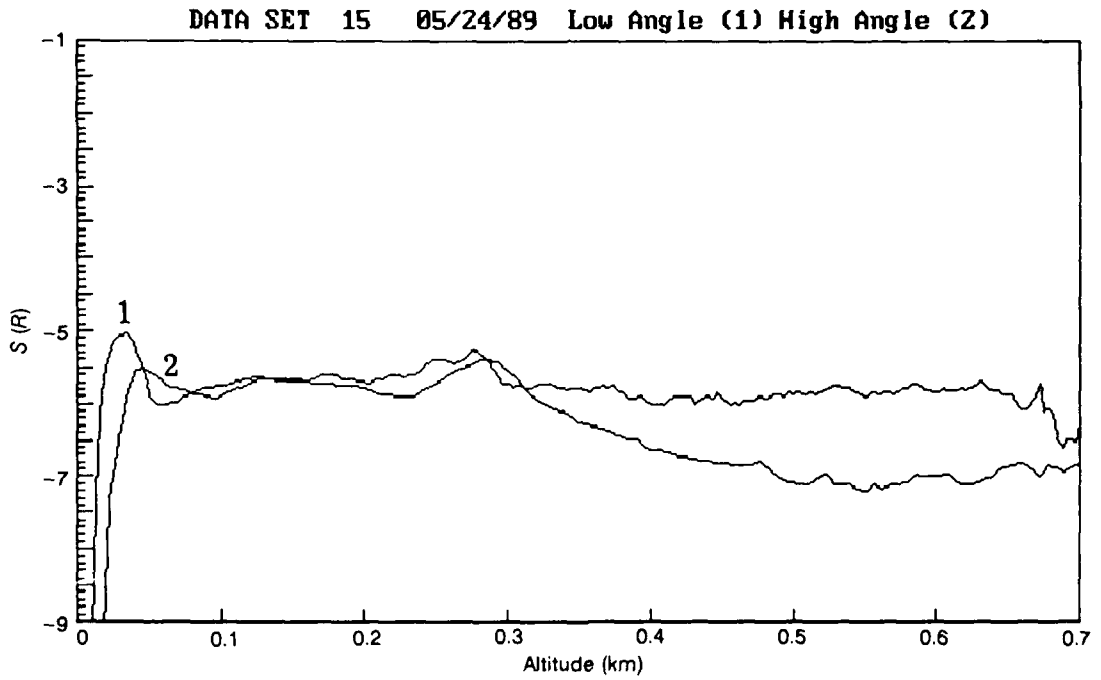

Figure A-1. Contd.